Kinetic Mechanism of DNA Polymerases:

Contributions of Conformational Dynamics and a Third Divalent Metal Ion

Austin T. Raper[†], Andrew J. Reed[†], and Zucai Suo[*]

Department of Chemistry and Biochemistry, Ohio State Biochemistry Program, The Ohio State University, Columbus, OH, 43210

[†]These authors contributed equally.

[*]To whom correspondence should be addressed. Tel: (614) 688-3706; Fax: (614) 292-6773; Email: suo.3@osu.edu

Abstract

Faithful transmission and maintenance of genetic material is primarily fulfilled by DNA polymerases. During DNA replication, these enzymes catalyze incorporation of deoxynucleotides into a DNA primer strand based on Watson-Crick complementarity to the DNA template strand. Through the years, research on DNA polymerases from every family and reverse transcriptases, has revealed structural and functional similarities, including a conserved domain architecture and purported two-metal-ion mechanism for nucleotidyltransfer. However, it is equally clear that DNA polymerases possess distinct differences that often prescribe a particular cellular role. Indeed, a unified kinetic mechanism to explain all aspects of DNA polymerase catalysis, including DNA binding, nucleotide binding and incorporation, and metal-ion-assisted nucleotidyltransfer (*i.e.* chemistry), has been difficult to define. In particular, the contributions of enzyme conformational dynamics to several mechanistic steps and their implications for replication fidelity are complex. Moreover, recent time-resolved X-ray crystallographic studies of DNA polymerases have uncovered a third divalent metal ion present during DNA synthesis, the function of which is currently unclear and debated within the field. In this review, we survey past and current literature describing the structures and kinetic mechanisms of DNA polymerases from each family to explore every major mechanistic step while emphasizing the impact of enzyme conformational dynamics on DNA synthesis and replication fidelity. This also includes brief insight into the structural and kinetic techniques utilized to study DNA polymerases and RTs. Furthermore, we present the evidences for the two-metal-ion mechanism for DNA polymerase catalysis prior to interpreting the recent structural findings describing a third divalent metal ion. We conclude by discussing the diversity of DNA polymerase mechanisms and suggest future characterization of the third divalent metal ion to dissect its role in DNA polymerase catalysis.

Table of Contents Graphics

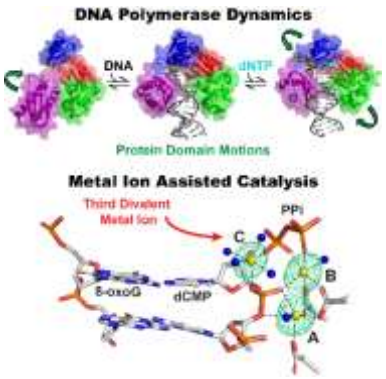

Table of Contents

1. Introduction

It is well-known that enzymes evolved for catalysis on nucleic acid substrates often undergo conformational dynamics and engage metal ion cofactors to achieve remarkable catalytic efficiency and reaction specificity.[1-14] In fact, replication of valuable genetic material is entrusted to DNA polymerases, which utilize divalent metal ions to catalyze DNA synthesis. Since their initial discovery in 1950s,[15,16] many DNA polymerases have been identified and phylogenetically classified into distinct A, B, C, D, X, Y, and reverse transcriptase (RT) families based on sequence homology as well as functional and structural analyses.[8,17,18]

As DNA polymerases catalyze the same fundamental reaction (*i.e.* incorporation of deoxyribonucleotide (dNTP) into a nascent DNA primer strand), one could expect these enzymes to share a unified kinetic mechanism describing DNA binding, nucleotide binding, and nucleotide incorporation. However, functional studies have revealed that each polymerase family is often suited to a particular cellular role[19,20] as evident through the utilization of distinct DNA substrates (*i.e.* primer-template DNA, gapped DNA, damage-containing DNA, single-stranded DNA, *etc.*) and wide-ranging nucleotide substrate specificities, which result in varying DNA replication efficiency and fidelity.[8,20-26] Indeed, while some mechanistic steps remain common among DNA polymerases, researchers have uncovered several events that seem unique to a particular polymerase, or more broadly, a polymerase family. These events are often related to conformational dynamics and may prescribe distinct properties to the polymerase, which dramatically influence DNA and nucleotide binding as well as nucleotide incorporation. In fact, there is substantial debate about the involvement of a particular conformational change in the rate-limiting step of single-nucleotide incorporation and how this step may influence the fidelity of DNA polymerization.[4-6,20,27-29] In this review, we will describe the minimal kinetic mechanism for single-nucleotide incorporation determined by extensive structural and functional studies

of DNA polymerases performed by our lab and many others over the last 30 years and we will emphasize the importance of DNA polymerase dynamics to the mechanism of DNA polymerization. Altogether, our comprehensive analysis of DNA polymerase kinetics has led us to the conclusion that a common kinetic mechanism, encompassing all DNA polymerases, likely does not exist and each enzyme should be considered independently.

A two-metal ion mechanism for enzymes that can act on the phosphodiester backbone of DNA or RNA was first postulated by Beese and Steitz in 1991 based on crystal structures of exonucleolytic substrate and product complexes within the active site of the 3′-5′ exonuclease domain of *Escherichia coli* DNA polymerase I (Pol I).[30,31] They postulated that the mechanism of exonucleolytic cleavage would extend to DNA polymerization with each divalent metal ion coordinating essential active site residues and substrate groups as well as providing necessary transition-state stabilization for DNA synthesis thereby reducing the activation energy and facilitating successful nucleotidyltransfer onto a DNA primer strand. Thus far, the putative roles of the two divalent metal ions during the DNA polymerase-catalyzed reaction have been well-established empirically through biochemical and structural investigations.[1-3,8,24-26,30-37]

Notably, this proposed two-metal ion mechanism (Figure 1A) has been heralded as "a mechanism for all polymerases" and draws support from the fact that many crystal structures of DNA or RNA polymerases in complex with nucleic acid and incoming nucleotide (E•DNA•dNTP or E•RNA•rNTP, ternary complex) contain two divalent metal ions in the polymerase active site.[2,26] In a striking example of evolutionary conservation, DNA polymerases from all families have been characterized to follow the same two-metal ion mechanism based on mutational analysis, structural studies, and kinetic investigation.[2,8,25,33,34] However, recent time-resolved (also known as time-lapse, time-dependent, or soak-trigger-freeze) crystallographic studies of the Y- and X-family DNA

polymerases, including human DNA polymerases η (hPolη)[38,39], β (hPolβ)[40-45], and μ (hPolμ)[46], have provided substantial evidence to compel an expansion of the two-metal ion mechanism to include a transient (*i.e.* not observed in all time-resolved partial reaction structures), third divalent metal ion, the precise role of which is currently debated (Figure 1B and C).[47,48]

In this review, we aim to briefly summarize the extensive evidence supporting the two-metal ion mechanism for DNA polymerization while highlighting the possibility of a third divalent metal ion and evaluating its involvement in catalysis as well as its biological purpose and significance. This will include a detailed synopsis of the seminal time-resolved X-ray crystallography findings over the last five years that have sparked renewed interest in the metal ion mechanism including discussion about the evidence, timing, and dynamic nature of the third divalent metal ion. As a result of its transient character, there is some inconsistency with the time at which the third divalent metal ion appears during the reaction with some groups reporting its occupancy during nucleotidyltransfer[38,39,42,45] and others reporting its appearance only in the product complex.[40,41,44,46] Thus, it is unclear if the third divalent metal ion serves a role in transition-state stabilization (Figure 1B), product release, catalysis of the reverse reaction (*i.e.* pyrophosphorolysis, Figure 1C), or in modulating the chemical equilibrium of nucleotidyltransfer through product-state stabilization. A recent computational analysis of the third divalent metal ion with hPolη[49] supports roles in transition-state stabilization during the forward and reverse reactions. Similarly, our work with hPolβ[42,45] suggests a possible role in transition-state stabilization, while other structural and computational studies completed with hPolβ[40,41,44,50,51] and hPolμ[46] provide evidence for perturbation of the chemical equilibrium by inhibition of pyrophosphorolysis by the third divalent metal ion. Thus, the role of the third divalent metal ion is yet to be fully delineated, and may be unique for each polymerase or polymerase family. We will conclude with a short discussion of the implications that the third divalent metal ion has for the polymerase field

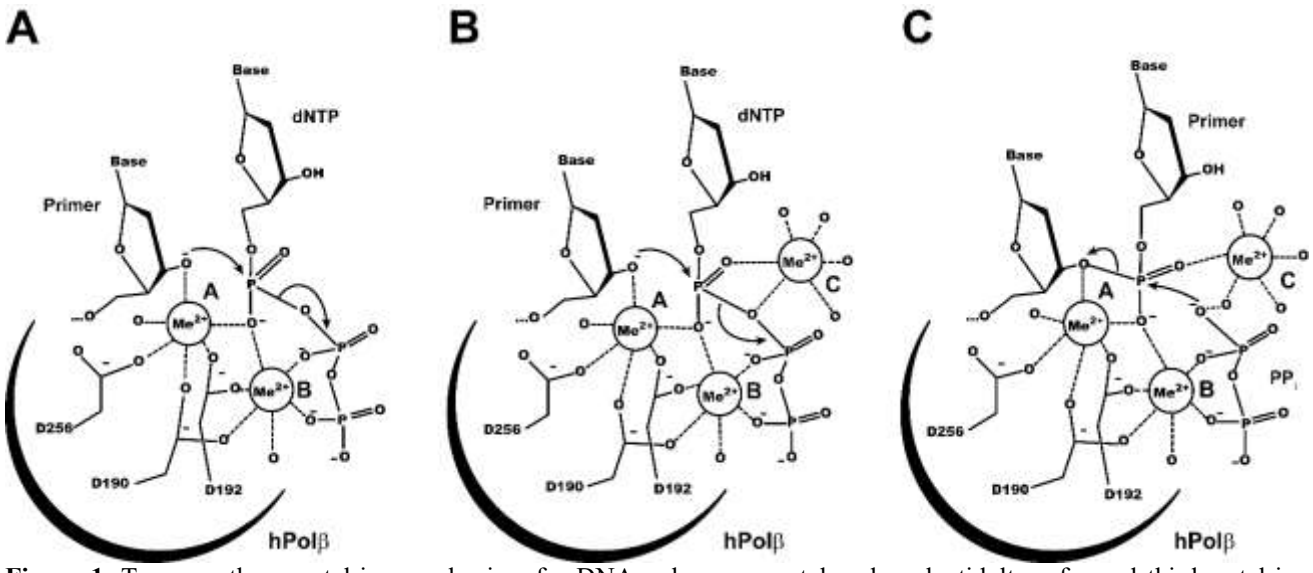

Figure 1. Two- vs. three-metal-ion mechanism for DNA polymerase-catalyzed nucleotidyltransfer and third-metal-ion assisted pyrophosphorolysis. The active site of the well-studied hPolβ was selected to depict the metal ion-based chemical mechanisms. (A) Two-metal-ion mechanism. The 3′-OH of the primer is activated (*i.e.* deprotonated) for an in-line nucleophilic attack on the α-phosphate of the incoming dNTP. The α-phosphate is coordinated by two divalent metal ions (Me^{2+}). The catalytic metal ion at the A-site is also coordinated by the 3′-OH of the primer, active site carboxylate groups (Asp 190, 192, and 256), and a water molecule. The metal ion at the B-site is coordinated by active site carboxylates (Asp 190 and 192), a water molecule, and non-bridging oxygen atoms of the β- and γ-phosphates, to complete the α,β,γ-tridentate coordination of the dNTP. The A-site ion is suggested to activate the primer 3′-OH nucleophile and the B-site ion stabilizes the negative charge of the pentacoordinated transition state. (B) Three-metal-ion mechanism. The reaction proceeds as in (A) except that a third divalent metal ion at the C-site appears to perhaps stabilize the transition state, serve as counter-ion to the oxyanion of the PP_i leaving group to aid product release, or participate in the reverse reaction, pyrophosphorolysis. The C-site ion is coordinated by water molecules as well as non-bridging oxygen atom of the α-phosphate and the bridging oxygen between α- and β-phosphates. (C) Third-metal-ion assisted pyrophosphorolysis. The third divalent metal ion may serve a similar role as the A-site metal ion in (A) and (B) to assist in the deprotonation and subsequent stabilization of the O_1 of PP_i. This atom would then attack the nascent phosphodiester bond of the DNA backbone, and the primer 3′-hydroxyl would be protonated to restore the pre-catalytic active site of nucleotide incorporation.

including its potential role in the mechanisms of replicative polymerases or as a potential target for antiviral therapies.

2. DNA polymerases and DNA polymerization

For 5′–3′ nucleic acid synthesis, the terminal 3′-hydroxyl group of a DNA or RNA strand serves as a nucleophile to attack the *α*-phosphate of a dNTP or ribonucleotide (rNTP) to form a phosphodiester bond while releasing pyrophosphate (PP_i) as a byproduct (Figure 1). In effect, a phosphodiester bond is transferred from the nucleotide to the nascent nucleic acid strand (*i.e.* nucleotidyltransfer). This reaction is catalyzed by enzymes termed DNA/RNA polymerases which bind both DNA/RNA and nucleotide substrates. As DNA and RNA polymerases share certain structural and functional similarities, much of

the mechanistic discussion of DNA polymerases focused on in this review may also apply to RNA polymerases. However, for more detailed evaluations of RNA polymerase structure and mechanism, we point the interested readers to several insightful reviews.[52-56]

DNA polymerases take advantage of the specific shape and hydrogen bonding patterns of nucleobase pairs (*i.e.* A:T, G:C) to faithfully recognize and incorporate correct nucleotides during DNA synthesis.[23] In addition to following a conserved two-metal-ion mechanism for nucleotide incorporation (Figure 1A),[2,26] DNA polymerases of all families adopt a "right-hand" architecture (with the exception of the X-family members which are left-handed: hPolβ, hPolλ, hPolμ, and terminal deoxynucleotidyl transferase (TdT))[57] consisting of fingers, palm, and thumb subdomains (Figure 2).[8,33] Along with these core domains, DNA polymerases may possess auxiliary domains (Figure 2) which often help in the execution of a specific biological function. For example, i) members of the A- and B- families often demonstrate high base substitution fidelity during DNA synthesis partially due to their accessory 3′-5′ exonuclease domain, which removes the small number of incorrect nucleotides incorporated during DNA replication; ii) members of the X-family may contain a deoxyribophosphate lyase (dRPase) domain for processing DNA ends during DNA repair; and iii) members of the Y-family contain a little finger subdomain (also named polymerase associated domain (PAD)) thought to serve a role in damaged DNA binding. These unique accessory subdomains and biochemical characteristics outfit polymerases from a particular family for a specific biological function.[19] Thus, the faithful, efficient, and processive A- and B-family polymerases perform the bulk of leading and lagging DNA strand replication.[58] In contrast, the error-prone and distributive X-family and Y-family DNA polymerases function in DNA repair and DNA damage response, respectively. Thus, the cell has evolved specialized DNA polymerases to perform an array of diverse functions and activities.[19]

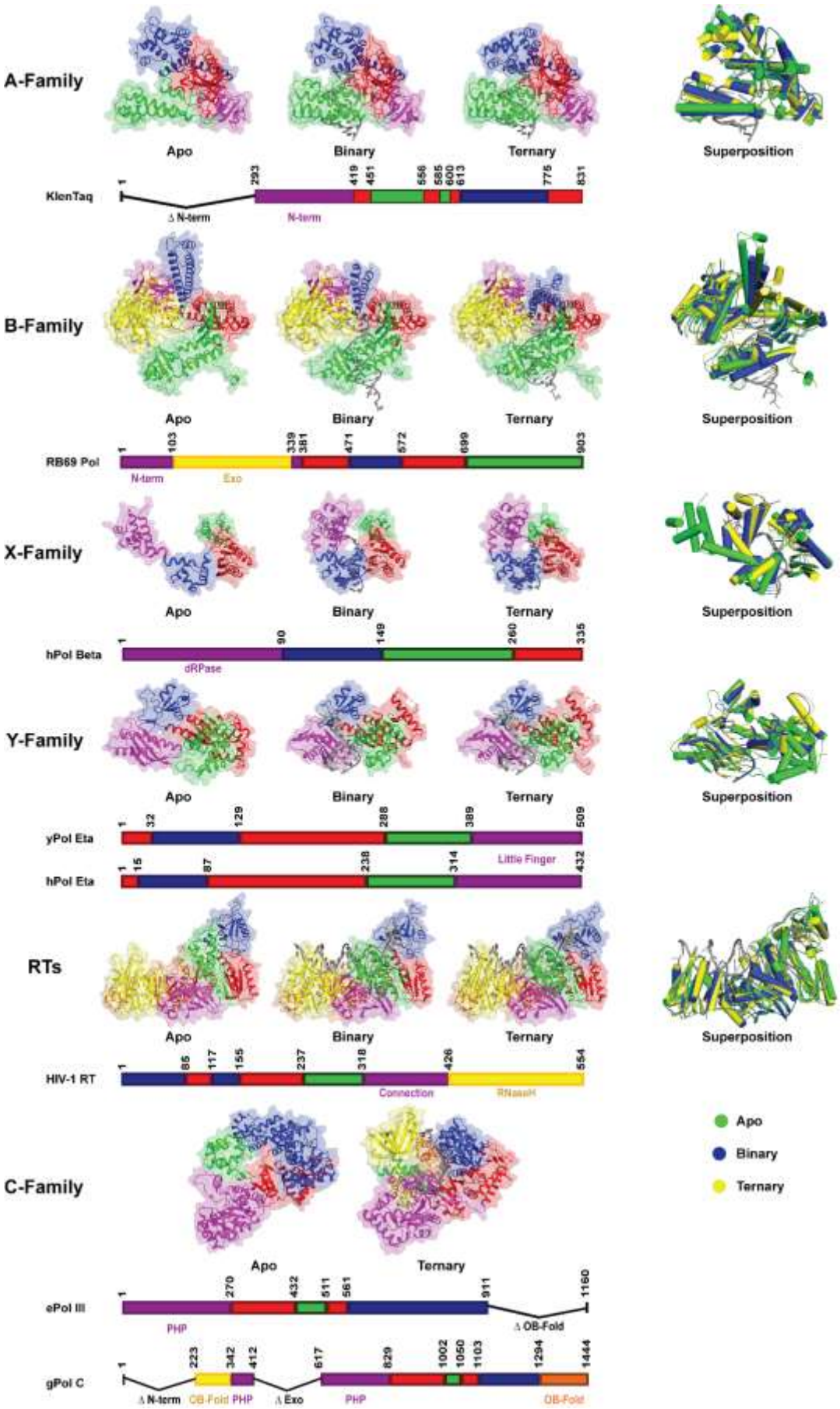
A-Family
Apo
Binary
Ternary
Superposition
KlenTaq
1
293
419
451
556
585
600
613
775
831
Δ N-term
N-term
B-Family
Apo
Binary
Ternary
Superposition
RB69 Pol
1
103
339
381
471
572
699
903
N-term
Exo
X-Family
Apo
Binary
Ternary
Superposition
hPol Beta
1
90
149
260
335
dRPase
Y-Family
Apo
Binary
Ternary
Superposition
yPol Eta
1
32
129
288
389
509
Little Finger
hPol Eta
1
15
87
238
314
432
RTs
Apo
Binary
Ternary
Superposition
HIV-1 RT
1
85
117
155
237
318
426
554
Connection
RNaseH
C-Family
Apo
Ternary
ePol III
1
270
432
511
561
911
1160
PHP
Δ OB-Fold
gPol C
1
223
342
412
617
829
1002
1050
1103
1294
1444
Δ N-term
OB-Fold
PHP
Δ Exo
PHP
OB-Fold
Apo
Binary
Ternary

Figure 2. Structural comparison of DNA polymerase families. Structures of apo, binary (DNA bound, E•DNA), and ternary (DNA and nucleotide bound, E•DNA•dNTP) enzyme forms of representative polymerases from each family and superposition of all three forms. The Klenow fragment of *Taq* DNA polymerase I (KlenTaq) was used for A-family (1KTQ, 4KTQ, and 3KTQ), RB69 DNA polymerase (RB69 Pol) was used for B-family (1IH7, 2P5O, and 3NCI), rat DNA polymerase β (rPol Beta, apo) and human DNA polymerase β (hPol Beta, binary and ternary) were used for X-family (1BPD, 1BPX, and 4KLG), yeast DNA polymerase η (yPol Eta, apo) and human DNA polymerase η (hPol Eta, binary and ternary) were used for Y-family (1JIH, 3TQ1, 4ECX), HIV-1 reverse transcriptase (HIV-1 RT) was used for RTs (1DLO, 3KJV, 3KK2), and *E. coli* DNA polymerase III (ePol III, apo) and *Geobacillus kaustophilus* PolC (gPol C, ternary) were used for C-family (4JOM and 3F2D). Each structure is shown as cartoon with transparent surface rendering and individual domains colored. For all structures the thumb, palm, and finger domains are green, red, and blue, respectively. Accessory domains are uniquely colored and named in the associated line diagrams. For the binary and ternary structures, the DNA is shown as gray cartoon. In the ternary structures, the nucleotide is omitted for clarity. The superpositions are shown with cylindrical helices for simplicity of comparison with apo, binary, and ternary structures colored green, blue, and yellow, respectively.

To catalyze nucleotidyltransfer, DNA polymerases require divalent metal ion cofactors. The roles of these metal ions in catalysis were elucidated in early structures of the Klenow fragment of *E. coli* DNA polymerase I with single-stranded DNA and dTMP product bound to the 3′-5′ exonuclease domain.[30,31,37] As the enzymatic synthesis and decomposition of nucleic acid molecules are closely related processes, the two-metal-ion mechanism proposed for 3′-5′ exonuclease degradation was extended to DNA polymerization (Figure 1A). In the exonuclease active site, one divalent metal ion was coordinated by several carboxylate side chains of surrounding amino acids (Asp355, Glu357, and Asp501), a water molecule, and the 5′-phosphate of the primer terminus. An additional divalent metal ion was coordinated by Asp355, the 5′-phosphate of dTMP, and several water molecules. Through mutation of the coordinating residues to alanine it was determined that these metal ions serve distinct mechanistic roles. Interestingly, it was later discovered that the catalytic subunit of HIV-1 reverse transcriptase[59] (HIV-1 RT) shares the same "right-hand" domain architecture of Klenow fragment with finger, palm, and thumb domains arranged to form the DNA binding cleft. Moreover, three conserved carboxylate amino acids identified in Klenow fragment were found in HIV-1 RT and their mutation to Ala also abolished catalytic activity.[59] Together, these data strongly supported the two-metal-ion mechanism for phosphoryltransfer reactions, including phosphodiester bond formation and degradation (Figure 1A).[60]

This two-metal-ion mechanism for DNA synthesis was later exemplified through the structure of rat DNA polymerase β, an X-family member, bound to primer-template DNA and dideoxy-terminated nucleotide (ddNTP).[61] From this structure, and those of rat DNA polymerase β bound to Mn^{2+} and dATP,[62] a common nucleotidyltransfer reaction mechanism involving two divalent metal ions for all DNA polymerases was postulated (Figure 1A).[61] Following polymerase binding at the primer-template junction of a DNA substrate, an incoming nucleotide is bound and positioned in the active site by i) Watson-Crick base-pairing with the templating base; ii) intermolecular contacts between the base, sugar, and phosphates with amino acid residues; and iii) coordination of two divalent metal ions by the three carboxylate residues. One metal ion binds between the primer terminal O3′ atom and the α-phosphate of the incoming dNTP and is often referred to as the A-site (M_A) or catalytic metal ion (Figure 1A). The second metal ion is coordinated by the incoming dNTP through the non-bridging oxygen atoms of the α-, β-, and γ-phosphates and is often referred to as the B-site or nucleotide binding metal ion (M_B) as its appearance coincides precisely with the binding of nucleotide (Figure 1A). During catalysis, M_A serves as a Lewis acid to lower the pK_a of the primer hydroxyl proton for abstraction and subsequent in-line nucleophilic attack on the α-phosphate of the dNTP to form a pentacoordinated transition-state with the 3′-oxygen of the primer terminus and four oxygen atoms of the α-phosphate, including one from the PP_i leaving group, occupying each position of the trigonal bipyramid. On the other hand, M_B acts to orient the triphosphate moiety of the bound nucleotide for catalysis and destabilizes the ground state ternary complex of the polymerase to promote catalysis. Furthermore, following nucleophilic attack, M_B stabilizes the pentacoordinated transition-state and neutralizes the developing negative charge on the PP_i leaving group (Figure 1A).[2]

Support for the two-metal-ion mechanism of DNA polymerization exists for structurally characterized DNA polymerases from all major families including A,[63-66] B,[67-70] C,[71-74] X,[40,61,62,75-79] and

Y[38,80-86] as demonstrated through ternary complex structures of enzyme, DNA, and dNTP with bound divalent metal ions (Figure 3). For example, the structures of bacteriophage T7 DNA polymerase[63] as well as *Thermus aquaticus* (*Taq*) DNA polymerase I[64] of the A-family, with DNA, ddNTP, and both divalent metal ions bound, were solved and are consistent with the earlier structural and mechanistic findings with rat DNA polymerase *β*.[61,62] Crystal structures of the replicative B-family DNA polymerases, including the bacteriophage polymerases T4[67] and RB69[68] also support the two-metal-ion mechanism. Consistently, two metal ions are also found in the active sites of repair and damage bypass DNA polymerases as demonstrated through crystal structures of rat DNA polymerase *β*,[36,37] discussed above, human DNA polymerase *λ* (hPol*λ*),[76] hPol*β*,[75,78] and hPol*μ*[77] of the X-family, as well as hPol*η*[80] and *Sulfolobus solfataricus* DNA polymerase IV (Dpo4)[87] of the Y-family.

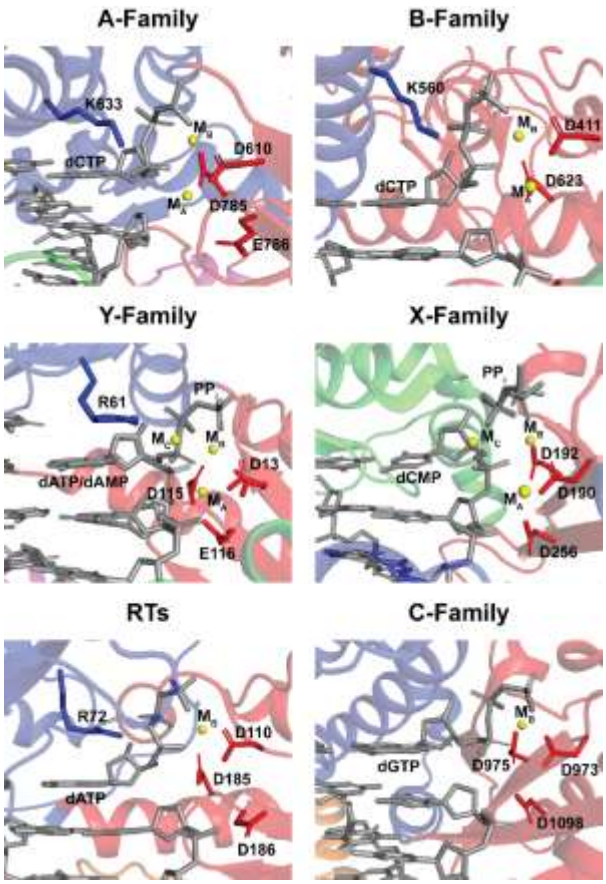

Figure 3. Active site comparison of DNA polymerases. Zoomed views of ternary structures of representative DNA polymerases from the A-family (KlenTaq, 3KTQ), B-family (RB69 DNA polymerase, 3NCI), the X-family (hPolβ, 4KLG), the Y-family (hPolη, 4ECX), the RTs (HIV-1 RT, 3KK2), and the C-family (*Geobacillus kaustophilus* PolC, 3F2D). The incoming/incorporated nucleotide (dNTP/dNMP+PP_i), DNA primer 3′-nucleotide, and active site carboxylates are shown as sticks. Metal ions bound at the active site are shown as yellow spheres. Importantly, in addition to the typical A- and B-site metal ions (M_A and M_B), the X- and Y-family structures have a third divalent metal ion bound (M_C). Many polymerases have positively charged residue side chains in the area where a third metal ion may bind and are shown as sticks in blue. Notably, *Geobacillus kaustophilus* PolC does not have a positively charged residue in this location.

Interestingly, RTs also engage two divalent metal ions for catalysis as demonstrated by the ternary crystal structure of HIV-1 RT.[88] Limited structural evidence from the C- and D-families of DNA polymerases is available as these enzymes are under-represented in the protein data bank. However, a

ternary complex crystal structure of a C-family polymerase from *Geobacillus kaustophilus*, as well as a lower resolution (4.6 Å) structure of *E. coli* PolIII*α*, suggest a two-metal ion mechanism for nucleotide incorporation.[71,73]

3. Kinetic and structural mechanism of DNA polymerases

Throughout the years, mechanistic studies of DNA polymerases from many diverse families, as well as reverse transcriptases, have culminated in a comprehensive kinetic pathway for nucleotide incorporation (Scheme 1A).[5,8-14,21-23,27,29,31,43,59,61,62,89-112] While particular details of this model may vary between DNA polymerases or systems (*i.e.* kinetically obligated removal or inclusion of elementary steps, see Scheme 1), we attest that the polymerase-catalyzed addition of correct nucleotides into a growing DNA primer strand occurs through ten steps (Scheme 1A). A DNA polymerase first binds a DNA substrate (Step 1, Scheme 1A) containing a primer-template junction to form the binary complex (E•DNA_n*, Scheme 1A), Initial DNA binding may place the terminal base pair of the DNA substrate within the polymerase active site (*i.e.* pre-insertion state) thereby occluding dNTP binding. However, DNA translocation (Step 2, Scheme 1A) by one nucleotide (E•DNA_n, Scheme 1A) to an insertion state correctly positions the templating base and creates the necessary space to bind an incoming dNTP in the subsequent step (Step 3, Scheme 1A). Notably, Step 3 includes the association of M_B and possibly M_A. Upon formation of this ground-state or loose ternary complex (E•DNA_n•dNTP, Scheme 1A), many polymerases then undergo a conformational change (Step 4, Scheme 1A) of the finger subdomain (or the thumb subdomain for the X-family DNA polymerases) which encloses the newly-formed base pair of the templating nucleotide and the incoming dNTP to form the tight ternary complex (E′•DNA_n•dNTP, Scheme 1A). A second conformational change (Step 5, Scheme 1A) within the polymerase active site generates the activated ternary complex (E″•DNA_n•dNTP, Scheme 1A) wherein reactive groups,

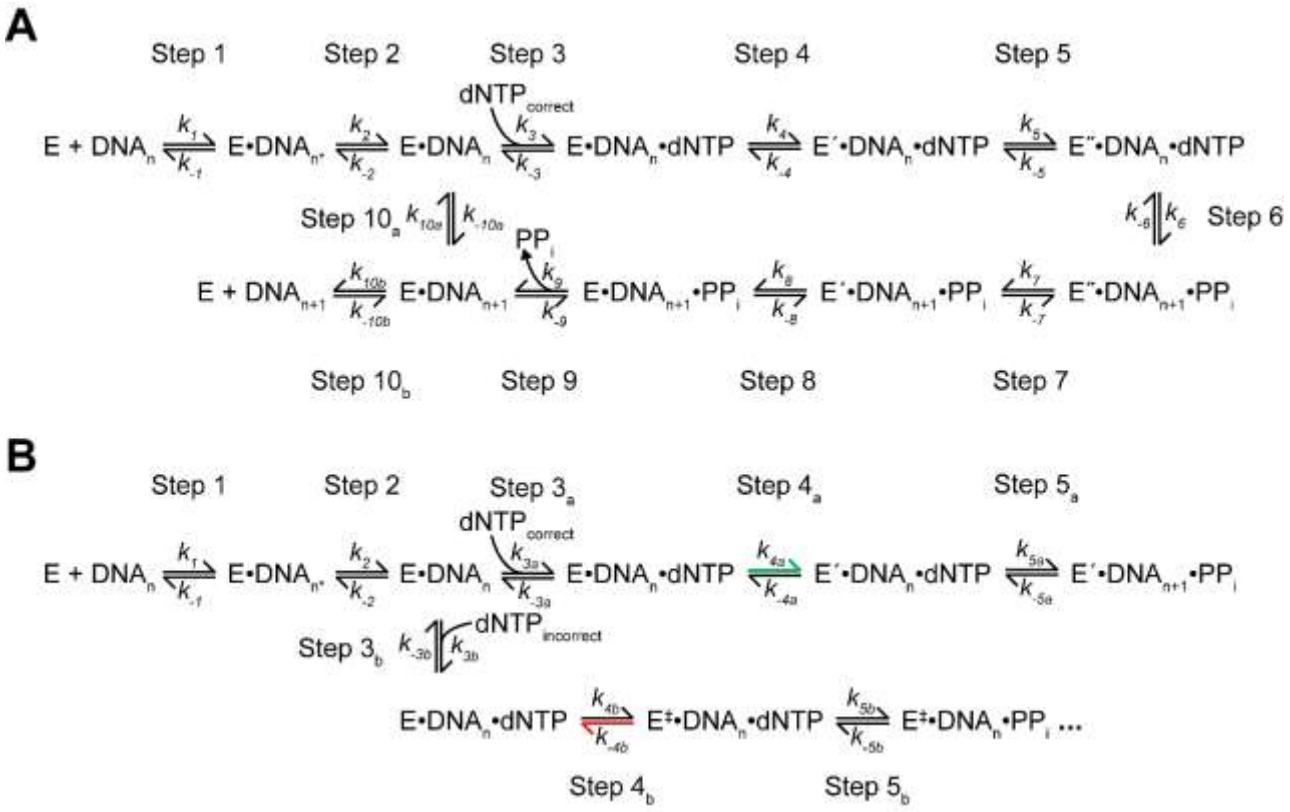

Scheme 1. Minimal kinetic mechanisms for nucleotide incorporation**.** (A) Kinetic mechanism of nucleotide binding and incorporation with E, E′, and E″ representing different conformations of the DNA polymerase with Step 5 representing an essential, rate-limiting conformational change. (B) Alternative kinetic mechanism wherein incorrect nucleotide is selected against by binding in a unique DNA polymerase conformation designated by $E^{‡}$. Steps 4_a and 5_a occur during correct nucleotide incorporation. Steps 4_b and 5_b occur during incorrect nucleotide incorporation. The green arrow in Step 4_a signifies that the forward rate is highly favored in the presence of correct nucleotide, where E and E′ represent a conformational change upon nucleotide binding. In the bottom branch, the red arrow in Step 4_b indicates that the reverse rate is highly favored in the presence of incorrect nucleotide. Following Step 5 the mechanism proceeds as in (A) for both correct and incorrect nucleotides. For (A) and (B) DNA_n^* signifies that the polymerase is bound to the DNA at the pre-insertion site (*i.e.* pre-translocated state).

including divalent metal ions, catalytic carboxylate residues, 3′-OH of the primer strand, and the α-phosphate of the bound nucleotide, are properly aligned for subsequent nucleotidyltransfer (Step 6, Scheme 1A), conventionally referred to as the chemistry step, which extends the primer strand by one nucleotide ($E''•DNA_{n+1}•PP_i$, Scheme 1A). The nucleotide-binding induced conformational changes (Steps 4 and 5, Scheme 1A) are reversed in Steps 7 and 8 (Scheme 1A) before PP_i is released (Step 9, Scheme 1A) from the polymerase active site. Following the reverse conformational changes and PP_i dissociation, the polymerase may translocate by one base pair along the DNA (Step 10_a, Scheme 1A) for

additional cycles of nucleotide incorporation (*i.e.* processive DNA synthesis) or may dissociate (Step 10_b, Scheme 1A) from the DNA substrate (*i.e.* distributive DNA synthesis).

3.1. DNA binding and associated polymerase dynamics

The inclusion and order of the elementary steps in Scheme 1A are strongly supported by kinetic, structural, and/or biophysical evidence. Logically, DNA binding (Step 1, Scheme 1A) occurs before dNTP binding as the templating information required for faithful replication is encoded in the DNA. This assertion is supported by inhibitor studies of nucleotide incorporation using PP_i,[24,113] as well as processivity assays, wherein DNA polymerases are observed to incorporate more than one nucleotide per DNA binding event.[90-92,94] In addition, ^{32}P-partioning experiments with *E. coli* Pol I indicated that the reaction followed a specific order in which the polymerase first associated with the DNA then bound dNTP.[114] Lastly, the relative affinity (*i.e.* K_d^{DNA}) of many polymerases for DNA is often in the sub-nanomolar concentration range, while binding affinities for correct or incorrect dNTPs (*i.e.* K_d^{dNTP}) often range from micromolar to millimolar concentrations. Accordingly, DNA polymerases likely spend disproportionately more time bound to DNA than to dNTP, increasing the likelihood of a strict order of substrate binding events. However, a recent structural and biochemical study of the X-family member hPolλ shows a preformed nucleotide binding pocket and reports relatively high affinities for dNTPs with a slight preference for dATP (3.3 μM for dATP and 15-45 μM for the other three dNTPs) in the absence of DNA. This suggests that the hPolλ may in fact bind Mg^{2+}-associated dNTP before DNA,[115] and helps to explain the higher base substitution frequency of hPolλ relative to hPolβ, a close X-family homolog.[109,116,117] While the ability of hPolλ to bind dNTPs prior to DNA is unusual, it has been structurally observed before[62,64,118-120] with the nucleotides often bound in a non-productive conformation. However, dNTP bound crystal structures of truncated hPolλ have shown productive binding of dNTP at the polymerase active site, but the global conformation of the protein has yet to

reach the catalytically active state in the absence of DNA.[115] Similarly, dNTP bound crystal and solution NMR structures (E•dNTP) of African swine fever virus (ASFV) Pol X, an X-family homolog, have revealed dGTP bound in a productive conformation that allows formation of *syn*-dGTP:dG Hoogsteen base pairs upon subsequent DNA binding,[118,121] which is different from the binding of nucleotide in multiple conformations shown for *Thermus thermophilus* Pol X.[122] Importantly, the structural results regarding this unique substrate binding order for ASFV Pol X have been confirmed by steady-state inhibition assays and nucleotide trapping assays.[123] Additionally, modeling based on chemical shift perturbations suggests that nucleotide binding to ASFV Pol X induces a conformational change in the absence of DNA, which further substantiates that dNTP binds first for this viral polymerase.[124] Nevertheless, the binding of nucleotide prior to DNA is likely a rare occurrence and may contribute to the low fidelity of Pol X.[125]

In addition, there may be certain scenarios in which the outcome of nucleotide incorporation is not influenced by the identity of the templating base. For example, a DNA polymerase may prefer to almost exclusively incorporate one particular nucleotide or catalyze template independent nucleotide incorporation such as the Y-family DNA polymerase Rev1, which is known to preferentially incorporate dCTP regardless of the templating base through a "protein template" arginine residue,[83,126-129] or the X-family DNA polymerase TdT, which prefers single-stranded DNA over double-stranded DNA and is incapable of replicating a DNA template,[23] respectively. Moreover, damage to the DNA may result in an unreadable templating base in which case a Y-family DNA polymerase is recruited for non-templated lesion bypass. Accordingly, while certain exceptions to the order of DNA and dNTP substrate binding to a DNA polymerase exist for specific biological contexts or for specialized DNA polymerases, it is widely accepted that DNA binding typically occurs prior to dNTP binding.

DNA polymerases have been observed to bind to a variety of DNA substrates and the substrate

specificity seems to depend on the polymerase family as well as the particular biological function. In general, it is understood that DNA polymerases bind primer-template DNA substrates wherein the 3′-end of the primer strand is recessed relative to the 5′-end of the template strand. However, specialized DNA polymerases such as hPolβ and hPolλ of the X-family prefer to act on gapped DNA substrates containing an upstream primer along with a 5′-phosphorylated or 5′-deoxyribophosphate adducted downstream primer,[79,116,117,130,131] and the Y-family polymerases can tolerate binding to and replicating on damage-containing DNA substrates,[132-139] unlike their replicative polymerase counterparts.[140-143] Several pre-steady-state kinetic assays exist to measure the equilibrium dissociation constant (*i.e.* K_d^{DNA}) for DNA binding by a polymerase including the active site titration. During the active site titration, a fixed amount of a DNA polymerase is titrated with varying amounts of a radiolabeled DNA substrate before being rapidly mixed with correct dNTP to initiate nucleotide incorporation.[144] A burst of product formation is observed at each DNA substrate concentration as dNTP is rapidly bound and incorporated by the pre-formed E•DNA (Scheme 1) complex. An important consideration for successful execution of the active site titration is that nucleotide binding and incorporation must be much faster than the binding equilibration of a polymerase and DNA (E + DNA ⇌ E•DNA), otherwise the burst of product formation will not be observed. The concentration of the E•DNA complex is given by the amplitude of the burst phase which varies as a function of DNA substrate concentration. A quadratic binding equation can then be used to determine both the K_d^{DNA} as well as the active concentration of the polymerase. For example, the DNA binding affinity of the catalytic subunit (*i.e.* p261) of human DNA polymerase ε (hPolε) of the B-family, which is responsible for leading strand DNA replication, was measured to be 79 nM and the enzyme was determined to be only ~16% active.[91] Interestingly, the assay was later repeated with the holoenzyme of hPolε (*i.e.* p261, p59, p17, p12) and the binding affinity increased 2.4-fold to 33 nM, while the enzyme did not gain appreciable activity (18% active).[145] In addition, active site titrations have

been useful in determining the DNA binding affinities of *Sulfolobus solfataricus* DNA polymerase B1 (PolB1)[92] and Dpo4[94] as both polymerase demonstrate clear burst phase kinetics. However, when a small or indeterminate burst phase is present, as observed for hPolβ,[110,146] the necessary conditions prescribed for an active site titration are not met (*i.e.* nucleotide binding and/or incorporation is not faster than the binding equilibration of a polymerase and DNA) and therefore a different method must be used to accurately measure DNA binding affinity. An alternative strategy to determine polymerase affinity to DNA involves measuring the microscopic rate constants of k_{off} and k_{on} comprising K_d^{DNA} (*i.e.* $k_{off}/k_{on} = K_d^{DNA}$) through assays designed to monitor the kinetics of polymerase dissociation from or association to a DNA substrate, respectively. Indeed, directly measured values for k_{off} and k_{on} often strongly agree with the measured K_d^{DNA} of a DNA polymerase and provide additional insight into mechanistic steps which may kinetically limit multiple rounds of DNA synthesis.[10,90-92,94,110,145,147,148]

Binding of a DNA substrate by a polymerase is often accompanied with conformational dynamics of the enzyme as well as nucleic acids (Figure 2). One striking example of protein dynamics upon DNA binding is demonstrated by *S. solfataricus* Dpo4 of the Y-family (Figure 4A). While in the apo state, a crystal structure of Dpo4 reveals that the auxiliary little finger domain interacts with the thumb domain and occupies the DNA binding cleft, thereby occluding the binding of a DNA substrate.[149] Consequently, a major 131° rotation and 1.7 Å translation of the little finger domain is observed in the binary complex crystal structure as the little finger breaks contact with the thumb and establishes new contacts with the finger to vacate the necessary space for DNA to bind (Figure 4A).[149] Additionally, high affinity of DNA binding[9,94,134] (K_d^{DNA} = 10 nM) is ensured as both the thumb and finger domains rotate 10° to better contact the DNA in the binary complex structure.[149] This dramatic structural transition was further investigated in fluorescence[149] and stopped-flow Förster resonance energy transfer (FRET) studies monitoring distance changes between[13] and within[10] individual Dpo4

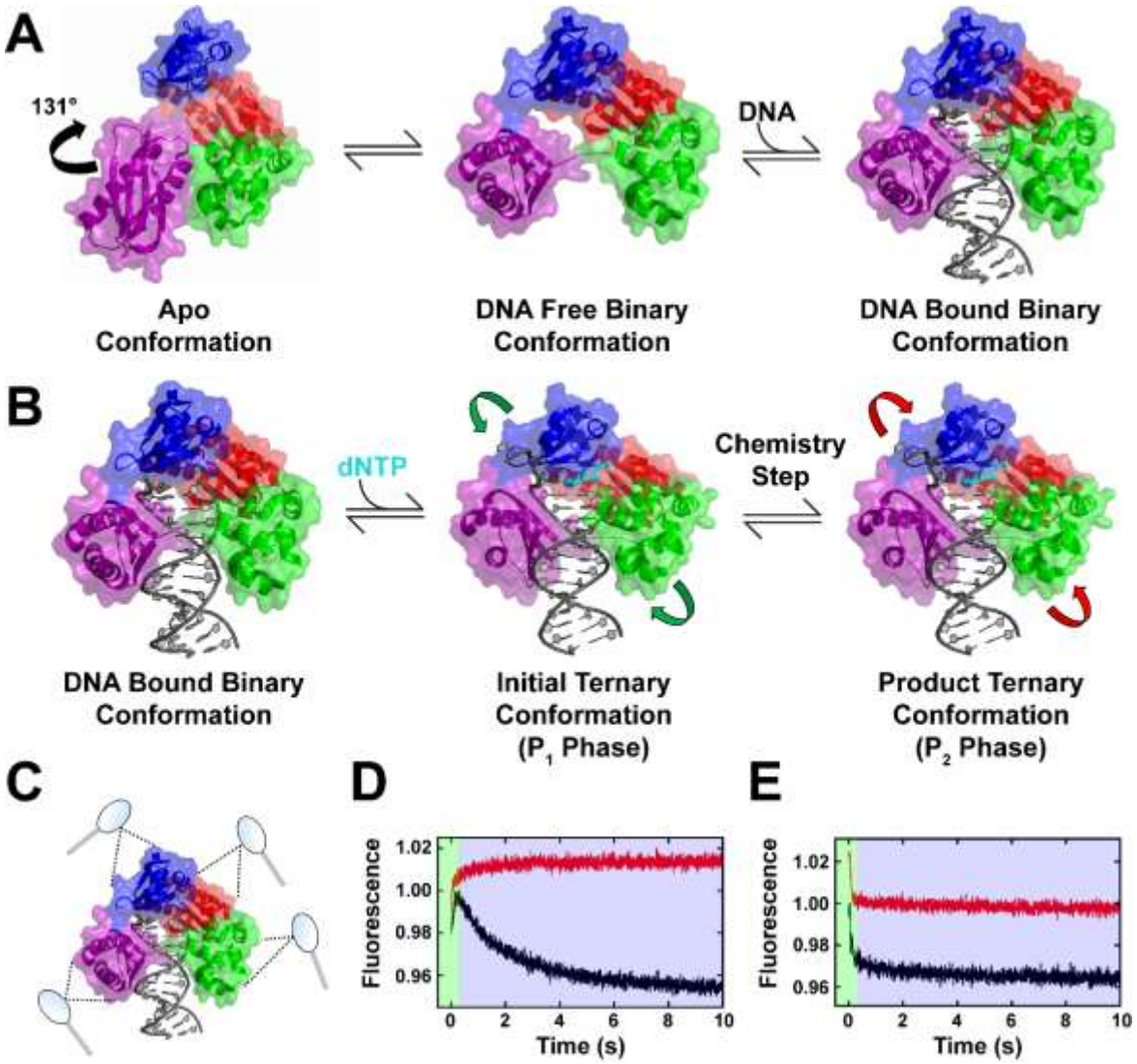

Figure 4. Conformational dynamics of Dpo4. Finger, palm, thumb, and little finger are colored blue, red, green, and purple, respectively. (A) Dynamics of DNA binding. Dpo4 exists in equilibrium between the apo and binary conformations in the absence of DNA. DNA binds to the free binary conformation which may be mediated by the little finger domain.[10,13] (B) Dynamics during nucleotide binding and incorporation. In contrast to A-, B-, and some X-family DNA polymerases, comparison of binary and ternary crystal structures of Dpo4 demonstrates a lack of significant nucleotide binding associated protein dynamics. However, stopped-flow FRET analyses have uncovered subtle motions for each domain of Dpo4. Green arrows indicate the concerted movement of domains upon nucleotide binding during P_1 phase to grip the DNA substrate. Red arrows depict the relaxation of domains during the P_2 phase (*i.e.* opposite direction of P_1) following nucleotide incorporation.[10-13] (C) Pictorial representation of the intradomain FRET approach to investigate Dpo4 conformational dynamics within each domain (represented by magnifying glasses). Trp residues were site-specifically introduced into each domain to serve as FRET donors, while Cys residues modified with 7-diethylamino-3-(4'-maleimidylphenyl)-4-methylcoumarin) were site-specifically introduced into each domain to serve as FRET acceptors.[10] (D) Stopped-flow trace of little finger intradomain FRET construct (Y274W-K329C^{CPM}). Black trace shows correct nucleotide binding and incorporation on a natural DNA primer and demonstrates characteristic, anti-correlated P_1 (green shaded area) and P_2 (blue shaded area) phases. Red trace shows correct nucleotide binding with a dideoxy-terminated primer.[10] (E) Stopped-flow trace of finger intradomain FRET construct (S22W-K56C^{CPM}) colored as in (D). Note the similar direction of P_1 and P_2 phases regardless of natural or dideoxy-terminated primer.[10] PDBs 2RDI and 2RDJ were used to generate the structural figures in (A), (B), and (C).[149]

1 domains. Contrary to the initial hypothesis that Dpo4 must follow an induced fit mechanism for DNA

binding, wherein the DNA substrate would induce the conformational change of the little finger domain, it was found that in the absence of DNA, Dpo4 exists in conformational equilibrium between the structurally distinct apo and binary complex configurations (Figure 4A) and DNA binding selects for the DNA bound state (*i.e.* shifts conformational equilibrium toward DNA bound state). This was concluded as the rate of conformational transition between apo and binary complex upon DNA binding, monitored through relative distance change between interdomain FRET probes positioned in the little finger and palm domains, was independent of DNA concentration over two orders of magnitude.[13] This assertion was supported by a nuclear magnetic resonance (NMR) study assigning the backbone chemical shifts of full length Dpo4 in the absence and presence of DNA, which suggested that a minor conformation of apo Dpo4 existed in a conformation consistent with that observed in the Dpo4 binary complex crystal structure.[150] Importantly, it was later shown that the little finger mediates initial DNA binding of Dpo4 through a stopped-flow FRET system reporting on intradomain distance changes of the little finger,[10] as predicted by a previous computational investigation.[151] A similar dramatic structural rearrangement is observed for the related Y-family member human DNA polymerase κ (hPolκ) during DNA binding as its little finger domain moves ~50 Å to intimately contact the DNA major groove and the N-clasp, a unique N-terminal extension, helps encircle the DNA substrate.[152] Conformational dynamics during DNA binding can also be observed for the X-family DNA polymerases hPolβ[61,62] and hPolλ,[76,115] but not hPolμ,[77,153] as the 8 kDa N-terminal dRPase domain of both hPolβ and hPolλ move to engage gapped-DNA substrates (Figure 2). Notably, subtle differences in the dRPase domain dynamics between hPolβ and hPolλ may help explain the higher affinity of hPolβ (0.077 – 22 nM)[146,154] for gapped-DNA relative to hPolλ (110 nM),[155] and its role as the primary polymerase for short-patch base excision repair (BER).[21] In contrast to the limited domain motion demonstrated by the X-family polymerases upon DNA binding, the gapped- (or nicked) DNA duplex undergoes a dramatic structural change involving a

90° kink occurring at the 5′-phosphodiester bond of the templating base.[79,153,156] Importantly, this unusual DNA structure is necessary for thumb domain closure during single-nucleotide gap-filling DNA synthesis by hPolβ and therefore ensures that an important fidelity checkpoint is maintained during nucleotide incorporation. Examination of product complex structures from enzymes involved in BER reveals that the DNA becomes progressively bent as it is sequentially bound and processed by most enzymes of the DNA repair pathway (DNA glycosylase → AP endonuclease → X-family DNA polymerase).[157] Accordingly, DNA repair enzymes may recognize and preferentially bind the bent DNA to facilitate rapid and efficient repair of DNA damage. The higher-fidelity A- and B-family DNA polymerases have also been observed to undergo conformational dynamics upon DNA binding as exemplified by comparison of the apo[158-160] and binary or ternary[64,65,68,161] crystal structures of bacteriophage RB69 DNA polymerase, *Pyrococcus furiosus* DNA polymerase, and *Taq* DNA polymerase I (Figure 2). In general, beyond the occasional structuring of disordered regions, DNA binding is typically accompanied by movement of the thumb (or the fingers for the X-family DNA polymerases) domain towards the palm domain in order to wrap around the DNA substrate.

3.2. DNA translocation and divalent metal-ion binding to the A- and B-sites

Following formation of the E•DNA binary complex (Step 1, Scheme 1A), nucleotide incorporation into the primer strand of the bound DNA substrate commences upon binding of a dNTP. Importantly, DNA polymerases in the binary complex may exist in non-productive or productive configurations depending on whether the polymerase active site is bound in the pre-insertion or insertion state, respectively. Indeed, a binary complex crystal structure of the Y-family member Dpo4 showed the polymerase in the pre-insertion state, while a ternary complex structure revealed the polymerase to have translocated by one base pair along the DNA to the insertion state in order to accommodate the incoming correct dNTP.[162] This essential DNA translocation event was later validated and measured to

be rapid (>150 s^{-1} at 20 °C) by stopped-flow[11,12] and single-molecule[9,163] FRET studies monitoring distance changes between a DNA substrate and various domains of Dpo4. Interestingly, the single-molecule FRET studies revealed that the polymerase dynamically fluctuates between the pre-insertion and insertion states on the DNA but exclusively populates the insertion state in the presence of correct nucleotide.[9,163] Similar repositioning of the DNA polymerase from the pre-insertion state to the insertion state via DNA translocation is proposed from crystal structures of the Klenow fragment of *Taq* DNA polymerase I[65] and the large fragment of DNA polymerase I from *Bacillus stearothermophilus*.[164] Indeed, as the polymerase transitions between these two states while bound to DNA (Step 2, Scheme 1), nucleotide may directly bind to the polymerase-DNA complex at the insertion site or may induce DNA translocation from the pre-insertion site depending on which state is favored at equilibrium.[112]

Once the polymerase has translocated along the DNA to the insertion state, nucleotide binding can commence (Step 3, Scheme 1). Binding of dNTP coincides with association of the A- and B-site divalent metal ions. Time-resolved crystallographic studies (Figure 5, see Section 4.1) of bacteriophage N4 RNA polymerase indicate that M_B binding occurs simultaneously with nucleotide binding and that M_A binding occurs shortly after.[165] This explicit order for divalent metal ion binding to the polymerase (*i.e.* M_B followed by M_A) is supported by the crystal structure of DNA polymerase ι (hPolι) wherein M_B is clearly associated with the bound dNTP but M_A has yet to bind.[82] However, those authors suggest that M_A may not be necessary for nucleotidyltransfer, as abstraction of the 3′-hydroxyl proton may occur by an active site carboxylate (Glu 127) positioned unusually near to the primer terminus.[82] In addition to binding after the M_B-associated nucleotide, M_A binding is proposed to occur following the conformational change (Step 4, Scheme 1A) to the tight ternary complex, as association of M_B-dNTP, not M_A, is sufficient to elicit the conformational change.[112,166-168] While this implies a defined order for the binding of each metal ion during the kinetic mechanism of DNA polymerase-catalyzed nucleotide

incorporation (Scheme 1A), explicit evidence for the defined sequence of events is lacking and M_A could associate or dissociate at different step(s) of the mechanism.[112] Nevertheless, time-resolved crystallographic studies of hPolβ[40-42,44,45] and hPolμ[46] (see Sections 4.4 and 4.5, respectively) have demonstrated that following nucleotide incorporation, M_A dissociates prior to M_B indicating that the relative affinity for the divalent metal ion at the A-site is weaker, and further suggesting that M_A likely associates after M_B.

3.3. Nucleotide binding, incorporation, and polymerase fidelity

The apparent affinity of the DNA polymerase binary complex for dNTP (*i.e.* K_d^{dNTP}) and the maximum rate constant of single-nucleotide incorporation (*i.e.* k_{pol}) can be experimentally measured by pre-steady-state kinetic assays.[144] Briefly, DNA polymerase and DNA substrate can be pre-incubated under single-turnover reaction conditions (*i.e.* [E] >> [DNA]) before mixing with various concentrations of correct or incorrect dNTP. Reactions are quenched at increasing amounts of time and the data are fit to a single-exponential equation ([product] = A[1 – exp(- $k_{obs}t$)]) to obtain an observed rate constant (k_{obs}) at each concentration of dNTP. The k_{obs} values are then plotted as a function of dNTP concentration and fit to a hyperbolic equation (*i.e.* $k_{obs} = k_{pol}$[dNTP]/(K_d^{dNTP} + [dNTP]) to obtain the desired kinetic parameters.[144] Importantly, the measured values of k_{pol} and K_d^{dNTP} for all 16 possible nucleotide incorporations are extremely useful metrics of polymerase efficiency (k_{pol}/K_d^{dntp}), fidelity (calculated as $(k_{pol}/K_d^{dNTP})_{incorrect}$ / [$(k_{pol}/K_d^{dNTP})_{correct}$ + $(k_{pol}/K_d^{dNTP})_{incorrect}$]), and processivity. This latter metric can be calculated as the ratio of k_{pol} to the rate of DNA dissociation (k_{off}, see section 3.1) and describes the average number of bases incorporated by the DNA polymerase during a single DNA binding event, which can be more than 1,500 as observed for highly-processive T7 DNA polymerase (bound to the processivity factor *E. coli* thioredoxin)[90] and human mitochondrial DNA polymerase γ holoenzyme,[169] or less than 20 as observed for the poorly-processive X-family member hPolβ[116] and the

Y-family member Dpo4.[94] Importantly, processivity values often increase when the DNA polymerase is associated with accessory subunits or processivity factors (*e.g.* proliferating cell nuclear antigen (PCNA) and β-clamp).[90,108,169-171]

Some of the fastest and most faithful-DNA polymerases exhibit k_{pol} values >200 s^{-1} and bind correct nucleotide with relatively high affinity ($K_d^{dNTP} < 10\ \mu M$), while incorrect nucleotides are bound with ~10- to 100-fold lower affinities and are generally incorporated 100- to 10,000-fold more slowly. Consequently, high fidelity polymerases typically make only one error per ~1 x 10^6 incorporations.[112] For example, the p261 catalytic subunit of hPolε was shown to incorporate correct nucleotides at a rate of 219 – 275 s^{-1} with a high base substitution fidelity of 10^{-4} – 10^{-7} (*i.e.* one error per 10^4 – 10^7 incorporations).[172] More impressively, it was further shown that the 3′-5′ exonuclease activity of hPolε bolstered the overall *in vitro* polymerization fidelity to 10^{-6} – 10^{-11} (*i.e.* one error per 10^6 – 10^{11} incorporations), which unprecedentedly translates to 0.1 – 1 misincorporations per round of human genome replication.[172] This enhancement in overall *in vitro* polymerization fidelity afforded by the exonuclease activity was greater than that observed for the related B-family DNA polymerase PolB1, which demonstrated a two orders of magnitude improvement (*i.e.* 10^{-4} – 10^{-6} to 10^{-6} – 10^{-8}).[173]

For many years, the mechanism by which a DNA polymerase recognizes a mismatch and switches between polymerization and exonuclease modes in order to correct the mismatch remained unclear. It was thought that the exonuclease domain must proofread the nascent DNA for mistakes and, upon identification of a mismatch, must transfer the DNA duplex from the polymerase active site to the exonuclease active site.[95,174,175] This was hypothesized to be a dynamic conformational change between polymerization and editing modes of the polymerase as the distance between the active sites is relatively large (~60 Å *E. coli* Pol IIIα, ~40 Å for *Saccharomyces cerevisiae* Pol ε).[174] Nevertheless, a recent cryo-electron microscopy (cryo-EM) study has revealed the structural basis for mismatch correction by *E.*

coli Pol IIIα.[176] Rather than serving an active role as a "proofreader", the exonuclease domain is actually passive, with a terminal mismatch causing the DNA substrate to fray (as supported by NMR analysis of the DNA duplex) resulting in a distorted DNA conformation.[176] Accordingly, the mismatch is essentially self-correcting as the primer strand from the frayed DNA duplex travels ~55 Å to the exonuclease active site for passive nucleotide excision.[176] This passive mechanism of exonucleolytic cleavage is corroborated by biochemical studies of *S. cerevisiae* Pol ε wherein an extended β-hairpin loop motif, originally thought to serve an active role in mediating a switch between polymerization and editing modes, was shown to have no such effect.[177] Interestingly, relative to matched primer-template termini, the rate of primer extension from a mismatched terminus is slow relative to the rate of exonuclease excision allowing for efficient mismatch removal.[134,172,173,178,179] The structural basis for inefficient polymerization beyond a mismatch stems from a myriad of active site and DNA distortions that misalign reactive groups[180-184] even when the mismatch is several base pairs removed from the primer-template junction (*i.e.* mismatch position *n*-1 to *n*-4).[180] Moreover, binding of a correct nucleotide when the terminal base pair is a mismatch induces distinct structural alterations which ultimately deter nucleotidyltransfer.[184] Together, these structural determinants prevent misincorporations and subsequent extension and push the equilibrium to exonucleolytic removal of the errantly incorporated nucleotide. In contrast to high-fidelity DNA polymerases, moderate-fidelity DNA polymerases[185] such as the X-family members hPolβ and hPolλ lack exonuclease domains (Figure 2) and demonstrate poor base substitution fidelity on both non-gapped and gapped DNA substrates ranging from 10^{-2} – 10^{-5} (*i.e.* one error per 10^2 – 10^5 incorporations).[109,117,186,187] Similarly, the error-prone lesion-bypass Y-family DNA polymerases including hPolη[147,188] and Dpo4[93] also lack exonuclease domains (Figure 2) and display comparably poor base substitution fidelities of 10^{-2} – 10^{-4} on undamaged DNA substrates.

3.4. Kinetic basis for polymerase fidelity and the rate-limiting step of single-nucleotide

incorporation

The mechanistic basis by which DNA polymerases achieve their remarkable base substitution fidelity has been thoroughly investigated over the years. Based on the seminal findings of Watson and Crick,[189] it was originally thought that DNA polymerases would achieve high base substitution fidelity from the distinct hydrogen bonding patterns between correct versus incorrect base pairs. However, it was quickly discovered that hydrogen bonding alone could not explain the large difference in efficiency between incorporation of correct and incorrect nucleotides.[190] It was later suggested that both the shape of the nascent base pair within the polymerase active site as well as hydrogen bonding contribute to nucleotide specificity.[191-196] Alternatively, it was hypothesized that the difference in free energy between the chemistry of correct versus incorrect nucleotide incorporation alone could explain polymerase fidelity.[6] However, it has been shown that for many polymerases in which the kinetic mechanism has been thoroughly investigated that chemistry is not the rate-limiting step of correct nucleotide incorporation.[5] Accordingly, research now indicates that many factors including but not limited to hydrogen bonding, free-energy differences, base-pair shape complementarity, and polymerase conformational dynamics contribute to high-fidelity DNA synthesis.[5,6,196-198] In fact, even non-catalytic accessory domains[199] as well as the solvent accessibility and water network of a polymerase active site[200] have been implicated or directly shown to modulate polymerase fidelity. Furthermore, substrate dynamics have also been hypothesized to effect polymerase fidelity. For example, the rare tautomer hypothesis of polymerase fidelity postulates that replication errors occur at low frequencies due to the formation of high energy tautomers of DNA bases which allow incorrect base pairs to form Watson-Crick-like geometries and mislead the polymerase to catalyze a misincorporation. This hypothesis has gained recent support from crystal structures of the *Bacillus stearothermophilus* DNA polymerase I large fragment bound to a dC:dA mismatch[201] and a mutant of hPolλ bound to a dG:dT mismatch,[202] as

well as through NMR spectroscopy of DNA duplexes containing site-specific mismatches, which revealed that sequence-dependent tautomerization and ionization of incoming nucleotides within the polymerase active site leads to misincorporations as originally suspected by Watson and Crick.[189,203,204] Moreover, DNA template dynamics associated with incorrect nucleotide incorporation have also been observed.[205] Lastly, DNA polymerases have been demonstrated to monitor base complementarity through sequence independent minor groove interactions.[206-208] Therefore, it is clear that polymerase fidelity is complex and is achieved through a vast array of polymerase and substrate interactions and dynamics.

3.4.1. A two-step binding model for DNA polymerase fidelity

Pre-steady-state kinetic studies coupled with pertinent crystal structures of DNA polymerases and RTs provided the first indication that enzyme conformational dynamics were important for the mechanism of DNA polymerization and polymerase fidelity.[4,5,29,61,63,65,68,88,90,209,210] Together, these studies helped define a two-step nucleotide binding mechanism (Scheme 1B) involving rapid equilibrium binding of dNTP (Step 3_a and 3_b, Scheme 1B) followed by an open→closed conformational change of the finger (or the thumb for the X-family DNA polymerases) (Step 4_a and 4_b, Scheme 1B), supported by comparison of binary and ternary complex structures for many DNA polymerases (Figure 2). If rate-limiting, this conformational change would provide the additional selectivity crucial for discriminating against incorrect dNTPs.[27] For many polymerases, kinetic data from experiments studying the incorporation of a S_p-dNTPαS, a nucleotide analog in which the pro-S_p oxygen of the α-phosphate has been substituted with sulfur, indicated that a conformational change, rather than the chemistry of nucleotidyltransfer, was rate-limiting for single-nucleotide incorporation as the sulfur elemental effect (*i.e.* the decrease in the rate of nucleotide incorporation when using α-thio-dNTP versus normal dNTP) was negligible.[5] Briefly, as the A- and B-site metal ions do not interact with the pro-S_p

oxygen of a dNTP, the substitution of this atom to sulfur allows kineticists to infer the identity of the rate-limiting step of nucleotidyltransfer from the magnitude of the change in the observed single-nucleotide incorporation rate. Accordingly, significant elemental effects of 4–11-fold (*i.e.* $k_{obs,\ dNTP}/k_{obs,\ Sp\text{-}dNTP\alpha S}$) were previously considered to indicate that chemistry is rate-limiting for DNA polymerase catalysis, whereas smaller values (*i.e.* < 2-fold) suggest that pre-chemistry conformational changes are rate-limiting.[5,94,103,211] Notably, while a significant sulfur elemental effect was not often observed for correct nucleotide incorporation, experiments performed with incorrect nucleotide frequently revealed that the chemistry step (Step 5_b, Scheme 1B) was rate-determining, presumably as a result of misaligned reactive moieties within the polymerase active site.[5] It is important to mention that the sulfur elemental effect is no longer considered a reliable diagnostic for the rate-limiting step of nucleotide incorporation as intermediate effects (*i.e.* 2–3-fold) are difficult to interpret, while large effects (*i.e.* >10-fold) are thought to arise from disruption of the geometry of the transition-state (*i.e.* steric effects) and therefore no longer exclusively report on the chemistry step.[5] Moreover, the pro-S_p oxygen of the α-phosphate of the incoming dNTP has been hypothesized to not serve a major role in transition-state stabilization and therefore its substitution with sulfur does not adequately probe the chemistry step.[6] More convincing than the sulfur elemental effect, were results obtained through the pulse-chase/pulse-quench experiment, wherein an increase in reaction amplitude of the pulse-chase compared to the pulse-quench is indicative of a rate-limiting pre-chemistry conformational change.[5,99] During the pulse-quench, a pre-incubated solution of polymerase and DNA is mixed with [α-^{32}P]-radiolabeled dNTP for varying amounts of time before quenching. The pulse-chase proceeds similarly, except that before quenching, an excess of cold dNTP is added to the reaction mixture. Accordingly, if a slow-to-form polymerase complex ($E'\bullet DNA_n\bullet dNTP$, Scheme 1B) accumulates before the chemistry step (Step 5_a or 5_b, Scheme 1B) then the chase with excess cold dNTP should cause an increase in reaction amplitude as the reaction is chased

forward (*i.e.* an [α-^{32}P]-dNTP-bound polymerase complex can form additional product rather than the [α-^{32}P]-dNTP dissociating out of the active site). Indeed, results of the pulse-chase/pulse-quench experiments for many DNA polymerases identified a rate-limiting pre-chemistry conformational change and supported the two-step binding mechanism for correct nucleotide incorporation.[4,5]

3.4.2. The open→closed conformational change is not rate-limiting

While the initial two-step model for nucleotide selection and incorporation was strongly supported by structural and kinetic data, it was later contested as the measured rate of the open→closed conformational transition (Step 4_a, Scheme 1B) for polymerases was too rapid to be considered rate-limiting.[7,27,212,213] As this model depended on the assumption that the rate of the open→closed conformational change (Step 4 , Scheme 1A and 1B) must be slow relative to the chemistry step (Step 6, Scheme 1A; Step 5, Scheme 1B) to afford nucleotide selection specificity, a revised interpretation of the model was necessary.[4] Indeed, studies of T7 DNA polymerase,[27,112] RB69 DNA polymerase,[196,214] and HIV-1 RT[215-217] showed that the rates of the pre-chemistry forward and reverse conformational changes for correct (k_{4a} and k_{-4a}, respectively, Scheme 1B) or incorrect nucleotide (k_{4b} and k_{-4b}, respectively, Scheme 1B) relative to the rate of chemistry (k_{5a} or k_{5b}, Scheme 1B) defined nucleotide specificity. Accordingly, binding of the correct nucleotide rapidly induces a conformational change (*i.e.* large k_{4a}, Scheme 1B) to an enzyme complex committed to catalysis (*i.e.* small k_{-4a} relative to k_{5a}, Scheme 1B), while binding of the incorrect nucleotide induces a unique conformational change to an enzyme complex ($E^{‡}$•DNA_n•dNTP, Step 3, Scheme 1B) which allows rapid release of the incorrect nucleotide (*i.e.* large k_{-4b} relative to k_{5b}, Scheme 1B). Altogether, kinetic analysis revealed that the controversy concerning the relative magnitudes of the rates of the pre-chemistry conformational change (k_{4a} and k_{4b}, Scheme 1B) versus the chemistry step (k_{5a} and k_{5b}, Scheme 1B), and how this could impact nucleotide specificity, was unfounded if the reverse rate of the pre-chemistry conformational change was slow for correct

dNTP (k_{-4a}, Scheme 1B), but fast for incorrect dNTP (k_{-4b}, Scheme 1B), relative to the chemistry step (k_{5a} and k_{5b}, Scheme 1B).[27,112,215,216] This current model suggests that chemistry is fast relative to nucleotide release during correct nucleotide incorporation as the rapid conformational change, promoted by the correct geometry of the base pair within the ground-state ternary complex (E•DNA•dNTP, Scheme 1B), ensures the proper alignment of catalytic moieties (E′•DNA_n•dNTP, Scheme 1B). On the other hand, chemistry is slow during incorrect nucleotide incorporation as a unique conformational change, prompted by the incorrect geometry of the base pair within the ground-state ternary complex (E•DNA•dNTP, Scheme 1B), instigates improper alignment of catalytic groups ($E^{‡}$•DNA_n•dNTP, Scheme 1B) and dissociation of nucleotide. In other words, the reversal of the pre-chemistry conformational change is fast relative to chemistry during incorporation of a mismatch, thereby favoring rapid nucleotide dissociation from the polymerase active site prior to nucleotidyltransfer as demonstrated through studies of high-fidelity T7 DNA polymerase[27,112] and RB69 DNA polymerases,[187,203] as well as moderate-fidelity HIV-1 RT.[215-217]

3.4.3. Multiple mechanisms of DNA polymerase fidelity

While the latter model (see Section 3.4.2)[27,112,196] elegantly explains how high-fidelity DNA polymerases achieve their remarkable substrate specificity for correct nucleotide, it may not extend to the low-fidelity X- and Y-family DNA polymerases. In contrast to the large structural change upon nucleotide binding observed for many A- and B-family DNA polymerases, involving closure of the finger domain,[210] all members of the Y-family[22,218] and some members of the X-family[57,115,153] do not undergo such a nucleotide-induced conformational change (Figure 2 and 4B). Despite the structural data, results from the sulfur elemental effect and pulse-chase/pulse-quench experiments for several Y-family DNA polymerases suggest that a pre-chemistry conformational change is rate-limiting for single-nucleotide incorporation.[22,94,103,104] Accordingly, the basis by which error-prone polymerases select for

correct nucleotide may involve a distinct mechanism.

Strikingly, stopped-flow fluorescence[219] and FRET[10-13] studies of the Y-family polymerase Dpo4 have revealed subtle conformational motions between and within each subdomain (finger, palm, thumb, little finger) during binding and incorporation of a correct nucleotide (Figure 4B and C). While monitoring distance changes between each polymerase domain and the DNA substrate, based on the anti-correlated increases or decreases in the donor and acceptor fluorescent signals, three FRET phases were observed upon mixing the polymerase-DNA binary complex with correct dNTP corresponding to i) rapid DNA translocation by Dpo4 (P_0), ii) synchronized gripping of the DNA substrate by each domain prior to nucleotide incorporation (Figure 4B, P_1), and iii) subsequent relaxation of each domain following nucleotidyltransfer (Figure 4B, P_2). Interestingly, the slow FRET phase (P_2) vanished during analogous experiments performed using a DNA substrate containing a dideoxy-terminated primer to prevent nucleotide incorporation and therefore must occur following nucleotidyltransfer. The P_1 phase (~15.3 s^{-1}) occurred much faster than the rate-limiting step of single nucleotide incorporation measured by radioactive chemical quench (0.66 s^{-1}). If the rate of synchronized domain motion (~15.3 s^{-1}) is considered the forward rate for enzyme isomerization (k_{4a}) in Scheme 1B, then the rate of chemistry (k_{5a}, Scheme 1B) can be calculated as 0.69 s^{-1} from the relationship $k_{5a} \approx k_{4a}k_{pol}/(k_{4a} - k_{pol})$,[27] where k_{pol} is the observed single-turnover rate for correct nucleotide incorporation (0.66 s^{-1}). In contrast to T7 DNA polymerase,[27,112] the forward isomerization rate (k_{4a}, Scheme 1B) for Dpo4 is much faster (22-fold) than the surprisingly slow calculated rate of chemistry (k_{5a}, Scheme 1B). Consequently, the reverse isomerization rate (k_{-4a}, Scheme 1B) must be much slower (0.0017 s^{-1} based on the 410-fold difference between forward and reverse isomerization rates measured for T7 DNA polymerase)[27] than 0.69 s^{-1} in order for Dpo4 to efficiently select the correct nucleotide according to the aforementioned revised model for nucleotide specificity (see Section 3.4.2 and Scheme 1B). However, given the clear lack of a sulfur

elemental effect (1.4) and obvious increase in amplitude (5.5 nM) for the pulse-chase compared to the pulse-quench experiment measured for Dpo4,[94] we hesitate to assign the chemistry step (k_{5a}, Scheme 1B) such a slow rate (0.69 s^{-1}) when it appears that some other rate-limiting, pre-chemistry step clearly exists. Indeed, previous kinetic studies of Dpo4 at a range of temperatures (2 – 56 °C) provided four independent lines of kinetic evidence that a pre-chemistry protein conformational change must limit correct nucleotide incorporation.[94,220] Accordingly, nucleotide incorporation for Dpo4 likely proceeds through a mechanism (Scheme 1A) requiring two pre-chemistry conformational changes (Steps 4 and 5, Scheme 1A). The first conformational change (Step 4, Scheme 1A) involves the synchronized domain movements to enhance interaction with the DNA substrate (Figure 4B), while the second (Step 5, Scheme 1A) is rate-limiting and involves precise alignment of reactive groups achieved through subtle protein motions. Indeed, stopped-flow FRET experiments monitoring distance changes between and within individual domains of Dpo4 during nucleotide binding and incorporation garner support for this model (Figure 4C).[10,13] For example, the majority of intradomain FRET pairs demonstrated characteristic P_1 and P_2 phases (*i.e.* anti-correlated phases consistent with interdomain FRET pairs, Figure 4B)[11,13] and the P_2 phase was absent during experiments with a dideoxy-terminated primer (Figure 4D). However, intradomain FRET pairs positioned within the finger domain showed a unique P_2 phase regardless if nucleotide incorporation was prevented by utility of a dideoxy-terminated primer (Figure 4E). Importantly, the unique P_2 phases were in the same direction as P_1 (Figure 4E) and the rates of these P_2 phases were on the order of the rate-limiting step of single-nucleotide incorporation measured for Dpo4 by ^{32}P-based assays. We speculate that the observed P_2 phases reflect subtle, collective domain motions necessary to align reactive moieties around the nascent base pair in preparation for rapid nucleotidyltransfer. Consistent with experimental results, these motions should occur whether or not phosphodiester bond formation is prohibited by a terminating primer[10] and may be

reflected in the fine adjustments of loops, secondary structural elements, and amino acid side chains near the nucleotide binding pocket as demonstrated through comparison of the binary and ternary crystal structures of Dpo4.[149] Experiments are currently underway to measure the reverse isomerization rate (k_{-4}, Scheme 1A) of Dpo4 in order to distinguish between the two competing mechanisms (see Sections 3.4.2 and 3.4.3) and identify how Dpo4 selects for the correct nucleotide. Future work will also determine how an incorrect nucleotide may affect the conformational dynamics of Dpo4. Importantly, an additional mechanism for nucleotide specificity by Dpo4 is based on hydrogen-deuterium exchange experiments suggesting that the DNA translocation step may be involved in correct dNTP selection as certain protein motions, speculated to occur during DNA translocation, are only observable in the presence of correct nucleotide.[221] Thus, correct nucleotide binding may stabilize the insertion state relative to incorrect nucleotide by slowing down Dpo4 reverse transition to the pre-insertion state. Similar to the latter model (Scheme 1B) for polymerase fidelity (see Section 3.4.2),[27,112] this suggests that nucleotide specificity hinges on a reverse step (*i.e.* reverse translocation, k_{-2}) being slow for correct dNTP, but fast for incorrect dNTP, relative to nucleotidyltransfer (Step 5, Scheme 1B). This model is supported by single-molecule FRET studies of Dpo4 showing that the correct nucleotide stabilizes the insertion state to a greater extent than incorrect nucleotide.[9,163]

Taken together, it is clear that the mechanisms by which DNA polymerases attain nucleotide specificity are complex and may vary significantly among the polymerase families. As a result, an overarching or unified mechanism to explain these intricate processes for DNA polymerases is likely not possible and we caution that what may appear true for one polymerase may not extend to all. A clear example of polymerase dependent selection mechanisms comes from our recent structural characterization of the inherent *D*-stereoselectivity of several DNA polymerases.[87,222,223] Through structures of the Y-family DNA polymerase Dpo4[87] and the X-family DNA polymerases hPolβ[222] and

hPolλ[223] bound to various nucleotide analogs with *L*-stereochemistry we identified several unique mechanisms by which these polymerases achieve *D*-stereoselectivity. While it was unsurprising that the Y-family polymerase Dpo4 and the X-family polymerases would not have common mechanisms of *D*-stereoselectivity, it was unexpected that hPolβ and hPolλ, which share a high amount of sequence and structural homology, select against *L*-nucleotides in different ways.[87,222,223] Thus, these studies highlight the difficulties in generating a unified mechanism for any aspect of DNA polymerase catalysis and support the necessity to study each polymerase individually.

3.5 Post-chemistry steps of nucleotide incorporation

Many biochemical, biophysical, and structural studies have aimed to deduce the kinetic mechanism and molecular bases for single-nucleotide incorporation and polymerase fidelity through characterization of the steps up to and including nucleotidyltransfer (Steps 1-6, Scheme 1A). However, post-chemistry steps involving the reverse (Steps 7 and 8, Scheme 1A) of the conformational changes observed during nucleotide binding and incorporation (Steps 4 and 5, Scheme 1A), as well as PP_i release (Step 9, Scheme 1A) have been seldom examined biochemically and/or structurally. Indeed, isolating post-chemistry events has proven to be difficult leading to the lack of sufficient structural and mechanistic characterization. As a consequence, the order in which PP_i release and the post-chemistry conformational changes occur as well as whether or not the events are cooperative (*i.e.* PP_i release triggers the reverse conformational change or vice versa) is unknown. However, recently the slow incorporation of nucleotide analogs, which closely resemble natural nucleotides but possess *L*-stereochemistry, has been utilized to capture *in crystallo* snapshots of post-chemistry events by hPolβ.[43] In performing time-resolved X-ray crystallography (see Section 4.1) with these analogs, the order of events following the chemistry step were unambiguously defined. Interestingly, hPolβ completed the closed→open conformational changes (Steps 7 and 8, Scheme 1A) while the product PP_i remained

bound to the polymerase active site. In fact, many of the side chain interactions with the PP_i were maintained despite the domain rearrangement, causing the PP_i to move with the thumb domain away from the incorporated nucleotide during the closed→open conformational transition. Presumably this reopening and movement of PP_i away from the reaction center would facilitate PP_i solvation and dissociation. Surprisingly, the third divalent metal ion previously identified in several time-resolved structural investigations[38-42] had already dissociated following domain reopening thereby directly opposing the hypothesis that the third divalent metal ion plays a role in PP_i dissociation (see Sections 1 and 4.3). Consistently, recent time-resolved X-ray crystallographic experiments with hPolμ in the presence of Mn^{2+} revealed that the third divalent metal ion dissociates prior to PP_i release and surprisingly showed that the B-site metal ion remains bound following PP_i release, rather than concomitantly dissociating with PP_i as previously purported.[46] Moreover, the post-chemistry structures of hPolβ demonstrate that the next correct nucleotide can bind to the open polymerase conformation to aid PP_i dissociation. This is not unexpected considering that if PP_i were to remain bound at the active site, then the incorporated nucleotide could be removed via pyrophosphorolysis. In this instance, one would expect concerted post-catalytic events including PP_i release, DNA translocation, and dNTP binding (*i.e.* Steps 9, 10_a, and 3, Scheme 1A). Altogether, rapid domain opening and the active displacement of PP_i by the incoming nucleotide ensures forward reaction efficiency during processive DNA synthesis.

In a recent study, PP_i mimetic analogs were used to follow the reverse reaction by time-resolved crystallography (see Section 4.1).[224] Consistent with the abovementioned structural findings that PP_i dissociation occurs after opening of the thumb domain,[43] this study demonstrated that during pyrophosphorolysis, PP_i binds to the open form of hPolβ and an open→closed conformational change occurs prior to the reaction.[224] Moreover, structures inform that PP_i fails to support binding of catalytic

Mg^{2+} at the A-site and is too far from the reaction center to promote efficient pyrophosphorolysis.[40] Consistently, biochemical and structural analyses with an imidodiphosphate PP_i analog demonstrated that a single atom change (*i.e.* bridging oxygen of PP_i substituted to nitrogen) allows optimal binding of catalytic M_A and positions the analog for efficient catalysis.[224] Interestingly, neither PP_i nor imidodiphosphate was efficient at removing mismatched primer termini, suggesting that pyrophosphorolysis does not act as a fidelity checkpoint during DNA synthesis.[224] Together, these studies have dissected the post-chemistry events of DNA polymerization and have shown that domain reopening occurs prior to PP_i release and the reverse reaction is highly disfavored.

4. New paradigm for DNA synthesis catalyzed by DNA polymerases

4.1. Time-resolved X-ray crystallography of DNA polymerase-catalyzed DNA synthesis

The ability to follow an enzymatic reaction at atomic resolution has been sought after for many years by biochemists and structural biologists.[225] Static crystal structures of complexes carefully designed to mimic reactant-, intermediate-, and product-states can, at best, only offer hints of the actual reaction mechanism. With the advent of time-resolved X-ray crystallography (Figure 5), much of the ambiguity that accompanies the interpretation of static crystal structures is replaced with clear insight into the chemical mechanism of a particular enzyme-catalyzed reaction. Generally, the technique involves preparation and isolation of a crystal containing an enzyme-substrate complex in a pre-catalytic state, followed by reaction initiation by transferring the crystal to a solution containing the reaction activator(s) and cryo-protectant (Figure 5A). Next, the reaction is allowed to proceed for a defined time interval before it is freeze-quenched by transferring the crystal to liquid N_2 (Figure 5A) for subsequent diffraction experiments. During generation of a structural model, the proportions (*i.e.* occupancies) of two or more states (*i.e.* reactant and product) are modeled and refined to fit the diffraction data (Figure

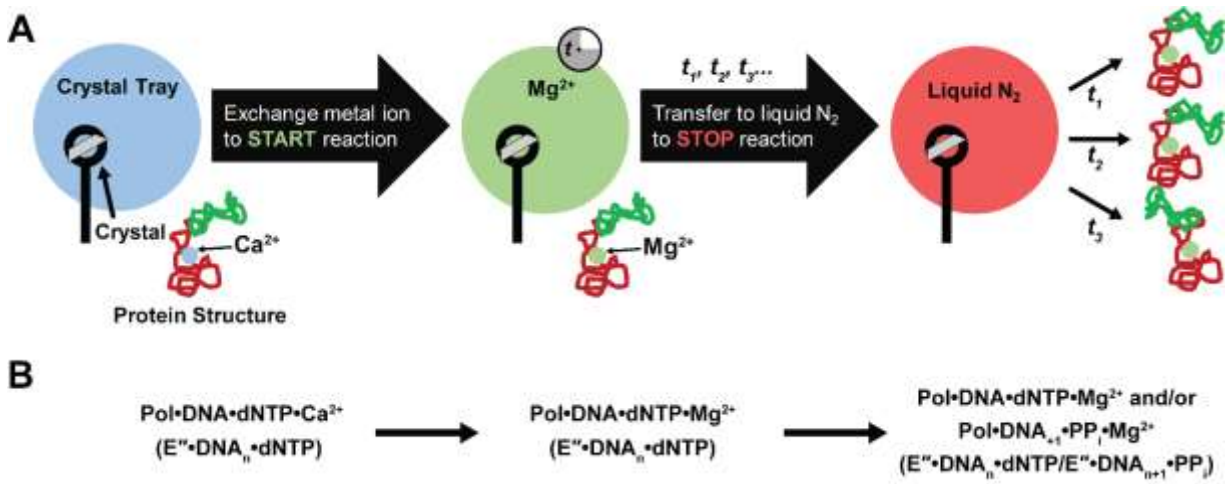

Figure 5. Time-resolved crystallography technique. (A) A crystal in a pre-reactive state is isolated and transferred to a cryo-solution containing the catalytic metal ion. This initiates the reaction *in crystallo* and after varying periods of time, the reaction can be quenched by transferring the crystals to liquid N_2. Diffraction experiments are then performed on the crystals and the diffraction data are used to determine the three dimensional structures. During this process, the electron density of the bond forming and of the bond breaking is modeled as percent occupancy. The F_o-F_c difference map is then used to evaluate how well the model satisfies the experimental electron density.[225] (B) For time-resolved crystallography of a DNA polymerase-catalyzed nucleotidyltransfer reaction, a crystal of the ternary complex formed in the presence of non-catalytic Ca^{2+} is transferred to a cryo-solution containing the catalytic divalent metal ion, Mg^{2+} or Mn^{2+}. The polymerase complexes relevant to panel (A) are depicted and the corresponding enzyme forms relevant to those shown in Scheme 1A are shown in parentheses. Reproduced from Raper, A. T.; Reed, A. J.; Gadkari, V. V.; Suo, Z. Advances in Structural and Single-Molecule Methods for Investigating DNA Lesion Bypass and Repair Polymerases. *Chem. Res. Toxicol.* 2017, 30, 260-269. Copyright 2017 American Chemical Society.

6). It is important to note that time-resolved crystallography is not a single-molecule technique. Rather, the average behavior of numerous molecules within the crystal, in the reactant- or product-states, contributes to the electron density at each time point. This process is repeated for several crystals, each allowed to react for an increasing amount of time. Finally, after solving the structure of the pre-catalytic complex (zero time point), the reaction progress from beginning to the end can be visualized, with each structure of a particular time point serving as a frame in the reaction film (Figure 7). For example, recent time-resolved crystallography with DNA polymerases (Figure 5) has been successful in following single-nucleotide incorporation[38-46] with an example of the modeling procedure applied during time-resolved crystallography of nucleotidyltransfer by hPol*β* shown in Figure 6 and example of the time-resolved snapshots captured by this technique depicted in Figure 7. Mechanistic events were able to be temporally resolved *in crystallo*, as reaction rates for single-nucleotide incorporation are observed to be

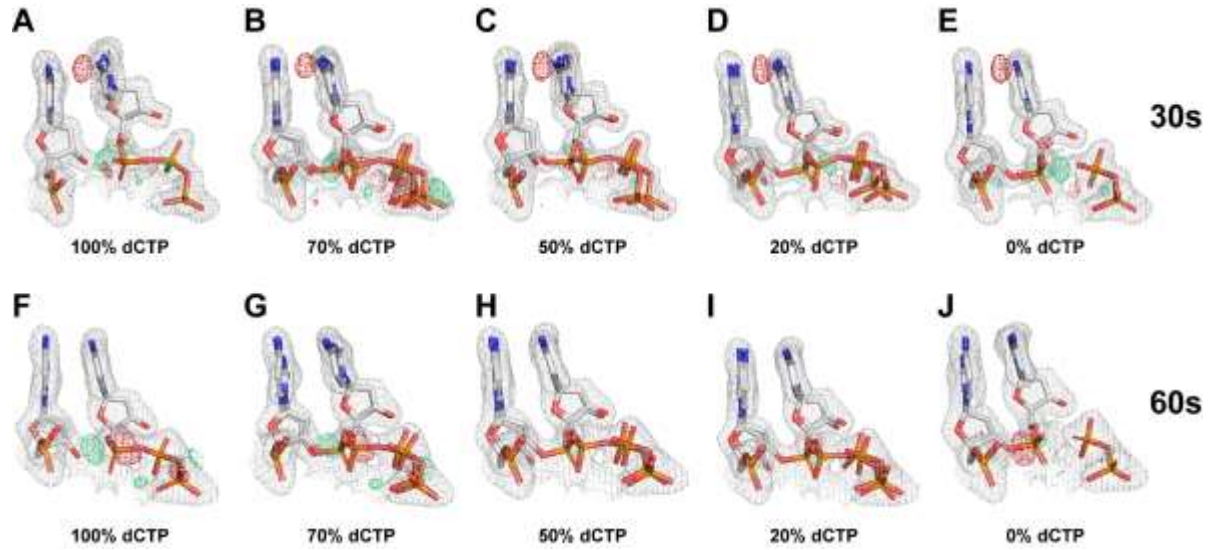

Figure 6. Modeling of phosphodiester bond formation after 30 or 60 s of Mg^{2+}/Ca^{2+} ion-exchange during time-resolved X-ray crystallography of hPolβ.[42] The $2F_o$-F_c (light blue) maps contoured at 1σ and the F_o-F_c omit maps contoured at either 3σ (green) or -3σ (red) are presented for the primer 3′-terminal nucleotide, incoming dCTP, incorporated dCMP, and PP_i. The modeled occupancy of the reactants is listed below each structure. Strong positive (green) and negative (red) electron density mesh between the primer 3'-OH and the α-phosphate group of dCTP or between the α- and β-phosphate groups of dCTP indicate unsatisfactory modeling, *e.g.* the modeling of the reactants at 100% (A), 70% (B), 20% (D) and 0% (E) occupancies for the 30 s structure and 100% (F), 70% (G), 50% (H), 20% (I), and 0% (J) occupancies for the 60 s structure. In contrast, the absence of any positive or negative electron density with the modeling of the reactants at 50% (C) and 20% (I) occupancies suggests satisfactory modeling for the 30 and 60 s structures, respectively.[42] Reproduced from Vyas, R.; Reed, A. J.; Tokarsky, E. J.; Suo, Z. Viewing Human DNA Polymerase Beta Faithfully and Unfaithfully Bypass an Oxidative Lesion by Time-Dependent Crystallography. *J. Am. Chem. Soc*. 2015, 137, 5225-5230. Copyright 2015 American Chemical Society.

20- to 100-fold slower for hPolη[38] and hPolβ,[40] compared to rates measured by pre-steady-state kinetic studies of these enzymes in solution.[38,104,226] To obtain these structures, the non-catalytic divalent metal ion Ca^{2+} was exploited to form a stable pre-catalytic complex (Figure 5B). Ca^{2+} was then exchanged for the catalytic divalent metal ions Mg^{2+} or Mn^{2+} to start the reaction (Figure 5B). Other unique properties of DNA polymerases made implementation of time-resolved X-ray crystallography successful including the relative ease of crystallizing pre-catalytic complexes, the ability to achieve high resolution diffraction data, and the limited impact of conformational heterogeneity or dynamics on crystal integrity during reaction progression.[225] While still a relatively new method (*e.g.* the first reports for DNA polymerases appeared only ~five years ago), researchers have already enjoyed success in utilizing the time-resolved structural technique to uncover new details of structure and function relationships of DNA polymerases. In the coming years, we expect that more details of the DNA polymerase mechanism,

1 extending beyond just the X- and Y-families, will be uncovered as more investigators adapt this

2 powerful methodology.

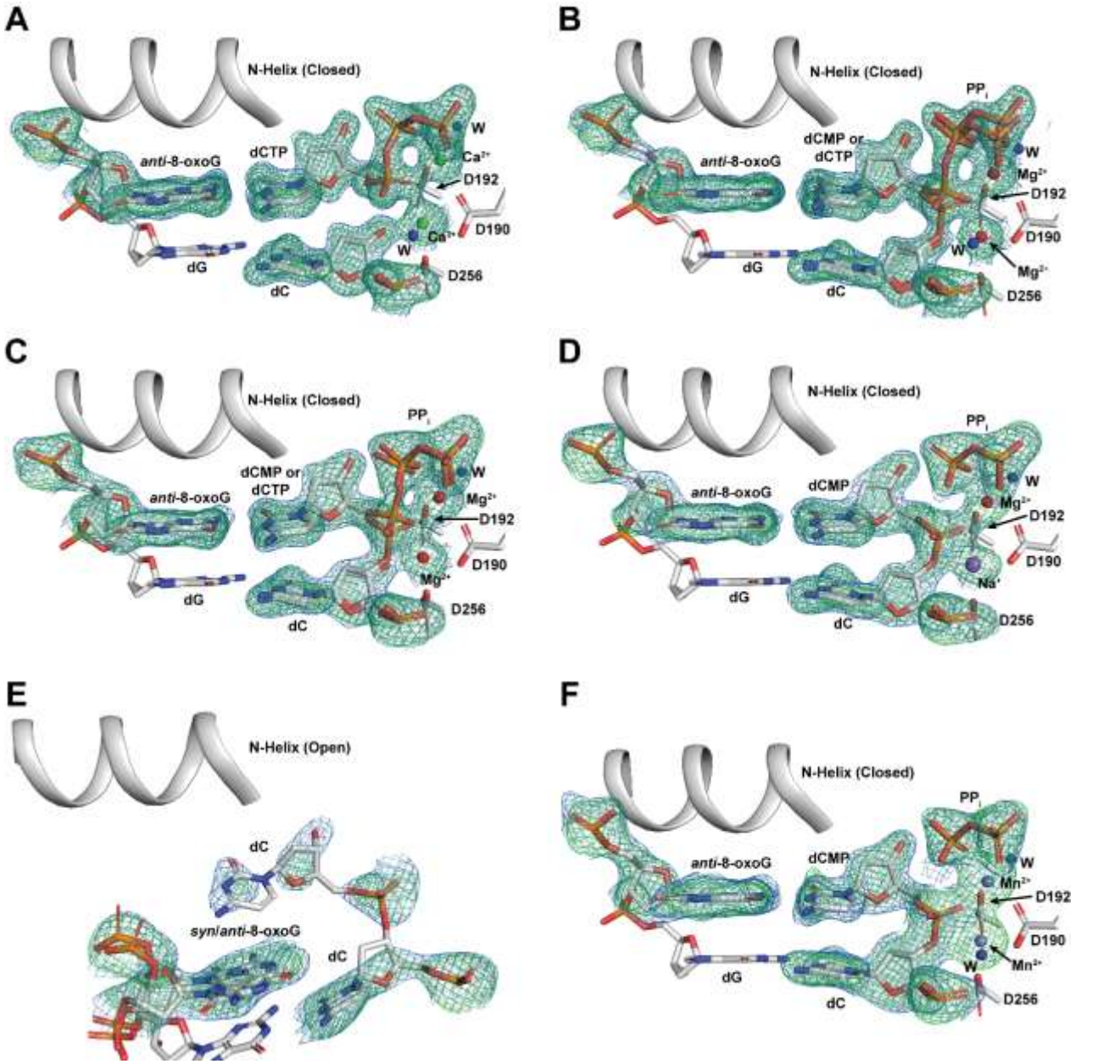

Figure 7. *In crystallo* phosphodiester bond formation by hPolβ. Zoomed active sites show the incorporation of dCTP opposite 8-oxoG. The $2F_o$-F_c (blue mesh) and F_o-F_c (green mesh) maps are shown for the templating 8-oxoG, incoming dCTP, incorporated dCMP, pyrophosphate (PP_i), metal ions at the A- and B-sites, and the primer 3′-terminal nucleotide (dC), contoured to 1σ and 3σ levels, respectively. Water molecules are shown as blue spheres. Ca^{2+}, Mg^{2+}, Mn^{2+}, and Na^{+} are shown as green, red, light blue, and purple spheres, respectively. Structures of the hPolβ pre-catalytic ternary complex (A), and structures of the hPolβ reaction intermediate or product ternary complexes following crystal-soaking with either 200 mM Mg^{2+} for 30 s (B), 60 s (C), 80 s (D), and 1 h (E), or 200 mM Mn^{2+} for 35 s (F). In (E), 8-oxoG was modeled in both *anti*- and *syn*-conformations.[42] Reproduced from Vyas, R.; Reed, A. J.; Tokarsky, E. J.; Suo, Z. Viewing Human DNA Polymerase Beta Faithfully and Unfaithfully Bypass an Oxidative Lesion by Time-Dependent Crystallography. *J. Am. Chem. Soc*. 2015, 137, 5225-5230. Copyright 2015 American Chemical Society.

4.2. A third divalent metal ion during nucleotide incorporation

Despite hundreds of structures of DNA polymerases accumulated through years in the Protein Data Bank, no evidence for a divalent metal ion directly involved in DNA synthesis beyond the well documented M_A and M_B divalent metal ions had been observed. However, the first time-resolved X-ray crystallographic investigation of hPolη,[38] as well as seven additional studies identify a transient, third divalent metal ion, referred to as the C-site (M_c) or product-associated metal ion, during phosphodiester bond formation (Figure 3).[39-46] Thus, traditional pre-catalytic substrate complexes and post-catalytic product complexes of DNA polymerases were not sufficient to structurally capture this apparently dynamic third divalent metal ion. High-resolution diffraction data (~1.5-2.0 Å) permitted for the unambiguous identification of metal ion electron density, coordination geometry, and metal ion-to-ligand coordination distances for M_C (Figure 8). Appropriately, M_C was shown to exhibit octahedral coordination geometry, consistent with a bound divalent metal ion, and short metal-to-ligand coordination distances (~2.2 Å), consistent with Mg^{2+} or Mn^{2+}, rather than non-catalytic Ca^{2+} (~2.4 Å). In some cases,[39-42] Mn^{2+} was used to initiate the *in crystallo* reaction, rather than Mg^{2+}, as its stronger signal (*i.e.* Mn^{2+} is more electron rich) allowed for confident assignment of M_C electron density even at 5σ levels (*i.e.* five standard deviations above background) (Figure 8D)[40,42] or resulted in anomalous diffraction.[40] M_C was shown to coordinate four water molecules as well as the non-bridging oxygen atom of the α-phosphate and the leaving oxygen atom of the β-phosphate (bridging oxygen between α- and β-phosphates) of the bound nucleotide (Figure 1B). In some instances, the number of ligands bound to M_C varied from four to six due to the dynamic nature of coordinating water molecules and presumably the transient nature of M_C. Importantly, these ligands fail to form any protein contacts, but only coordinate to the metal ion, therefore preventing any mutational confirmation of the existence or

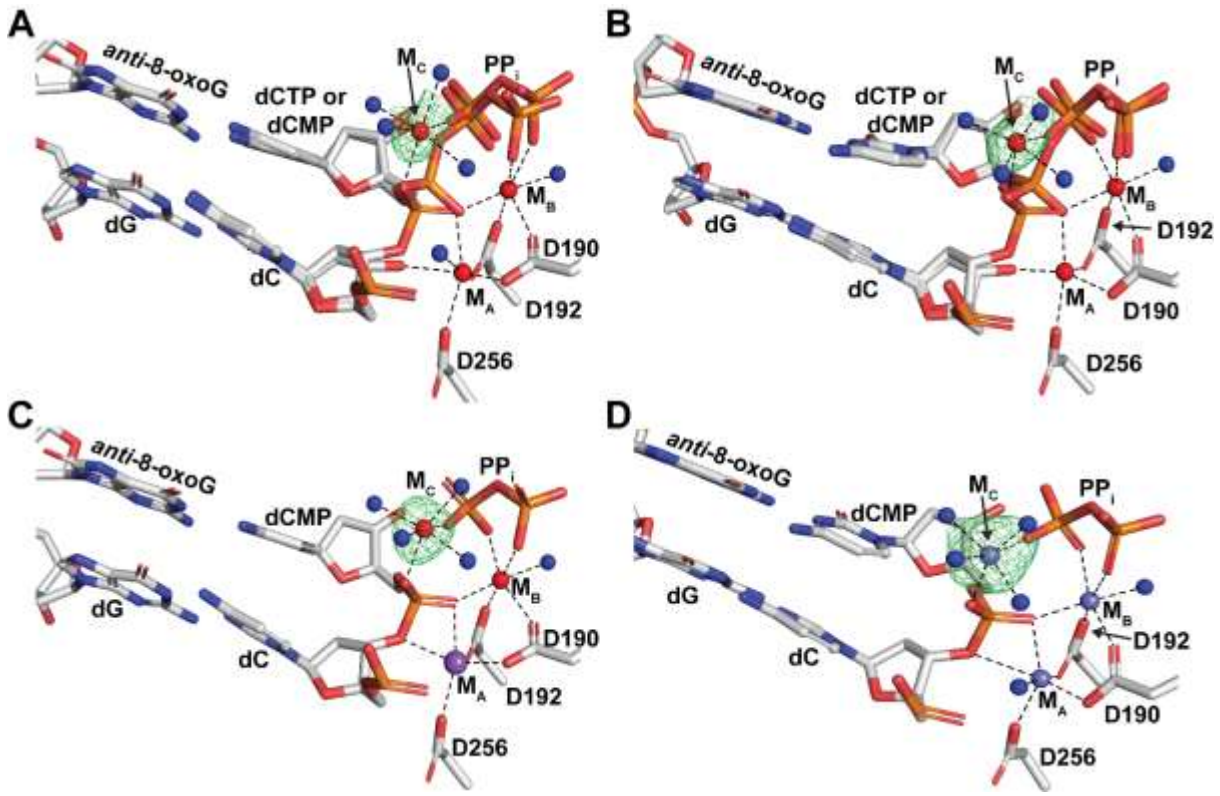

Figure 8. The third divalent metal ion is present in the reaction-state and post-catalytic structures of hPolβ during incorporation of dCTP opposite 8-oxoG. After soaking crystals of the pre-catalytic ternary complex of hPolβ (hPolβ•8-oxoG-DNA•dCTP) with Mg^{2+} for 30, 60, and 80 s, dCTP incorporation had completed by 50% (A), 80% (B), and 100% (C), respectively. (D) Following 35 s soaking with Mn^{2+}, dCTP was 100% incorporated. The F_o-F_c omit maps were contoured at 3σ (A-C) or 5σ (D) to show the electron density (green) of Mg^{2+} or Mn^{2+}, respectively, at the C-site. Coordinating aspartate side chains are shown as stick models, while water molecule ligands (blue), Mg^{2+} (red), Mn^{2+} (light blue), and Na^{+} (purple) are shown as spheres.[42] Reproduced from Vyas, R.; Reed, A. J.; Tokarsky, E. J.; Suo, Z. Viewing Human DNA Polymerase Beta Faithfully and Unfaithfully Bypass an Oxidative Lesion by Time-Dependent Crystallography. *J. Am. Chem. Soc*. 2015, 137, 5225-5230. Copyright 2015 American Chemical Society.

significance of M_C. Differences in the timing and occupancy of the third divalent metal ion amongst the time-resolved studies of hPolη,[38,39] hPolβ,[40-42,44,45] and hPolμ[46] are suggestive of its dynamic nature. Furthermore, a third divalent metal ion only appeared with hPolμ when Mn^{2+} was used for metal ion exchange and not with Mg^{2+}.[46] As a consequence of these inconsistencies, the role of the third divalent metal ion in the mechanism of nucleotide incorporation has been highly debated (Figure 1B and C) with hypothesized roles in transition-state stabilization, product release, catalysis of pyrophosphorolysis, or product-state stabilization.[46,47]

4.3. Evidence and hypothesized roles for the third divalent metal ion in single-nucleotide incorporation catalyzed by hPol*η*

In the inceptive time-resolved crystallography study, Nakamura *et al.*[38] followed nucleotide incorporation by hPol*η* and identified for the first time a third divalent metal ion utilized by a DNA polymerase during catalysis. M_C appeared midway through phosphodiester bond formation (140 s, 60% reactants, 40% products) and remained associated at the active site until the final recorded time point (230 s, 40% reactants, 60% product). Unfortunately, observation of full product and the subsequent release of PP_i was not observed as both the forward DNA synthesis and reverse pyrophosphorolysis reactions became competing at later time points as product occupancy decreased from the penultimate to the final time point. Furthermore, as the competing reactions were occurring simultaneously, it is likely that both activities were aided by M_C through transition-state stabilization and lowering the activation energy barrier for bond formation. Interestingly, appearance of M_C occurred concomitantly with the movement of a positively charged arginine residue (R61), which had flipped away from the *α*-phosphate of the bound dNTP, effectively replacing the charge in the active site. This active site configuration led to the hypothesis that the M_C would support chemistry while the subsequent reverse conformational transition of the arginine, or an equivalent positively charged residue in other polymerases, back to its pre-catalytic configuration would act in concert with the third divalent metal ion to actively displace product PP_i. In this way, the side chain is essentially "sweeping out" PP_i from the active site in preparation for DNA translocation and an additional catalytic cycle. Consistently, a molecular dynamics investigation of the pre-catalytic and reaction state side chain conformations of R61 concluded that only the pre-catalytic side chain configuration facilitates nucleotide binding, suggesting that the absence of nucleotide precludes reaction-state configuration. Moreover, following nucleotidyltransfer the side chain must revert back to the pre-catalytic configuration before subsequent rounds of dNTP binding and

incorporation.[49] Furthermore, the computational study maintained the notion that M_C, accompanied by the R61 conformational transition, serves as an exit shuttle for PP_i release, and dissociates along with PP_i.[49]

This mechanism of third divalent metal ion-dependent conformational transitions for nucleotide incorporation and product release may be conserved given that a lysine side chain in many polymerases from diverse families,[18,64,68,164,227,228] or an arginine residue in HIV reverse transcriptase,[88] is present at a position similar to R61 of hPolη. Alternatively, this positively charged side chain may be static and therefore occlude the binding of a third divalent metal ion and thus fulfil the roles of transition-state stabilization and/or PP_i release. Hence, it is necessary to investigate these other polymerase families or RTs through similar methods to determine the precise role of these amino acids and identify whether a third divalent metal ion is utilized. Notably, the X-family repair polymerases, hPolβ, hPolλ, and hPolμ, which typically act on single-nucleotide gapped DNA substrates (see Section 3.1), do not possess an analogous positively charged residue to interact with the α-phosphate. This may be a mechanism by which processive DNA synthesis is suppressed to prevent potential misincorporations by these moderate-fidelity enzymes.[79,146-148] While the Y-family polymerases, such as hPolη, are considered low-fidelity enzymes[22,147,229-231] (see Section 3.3), the necessity to bypass DNA damage and subsequently extend the DNA primer, which are both difficult tasks for high-fidelity replicative polymerases, may justify the need for the positively charged side chain to aid in processivity, in contrast to the X-family polymerases.

More recently a time-resolved crystallography study of hPolη directly investigated the role of M_C and suggested that it is absolutely essential for catalysis and its binding may kinetically limit the rate of single-nucleotide incorporation.[39] When crystals of the hPolη pre-catalytic ternary complex (E•DNA•dNTP•Ca^{2+}) were soaked with 1 mM Mn^{2+} for varying amounts of time, only the A- and B-site

metal ions were occupied by Mn^{2+} and no product formation was detected even after 1,800 s. However, after soaking the crystals in 10 mM Mn^{2+}, the A- and B- sites were readily occupied, while M_C appeared at 30 s coinciding precisely with the appearance of reaction product. The authors were able to determine the relative binding affinities for each metal ion from *in crystallo* metal ion titration experiments, where electron density for each metal ion was examined following crystal soaking at various metal ion concentrations and time points. It was determined that Mn^{2+} binds to the C-site with an affinity of ~3.2 mM. The apparent weak binding of M_C was further supported by in-solution metal ion titration experiments, wherein the concentration of metal ion necessary to achieve half-maximal reaction rate was determined and yielded a similar affinity (2.7 mM). Importantly, the agreement of the metal ion binding affinities from the two approaches (*i.e.* in-solution and *in crystallo* metal ion titrations) is the first experimental evidence to suggest that M_C is bound by hPolη in solution and is not simply a crystal artifact of the time-resolved crystallography technique.

Examination of the interaction of hPolη with S_p-dATPαS demonstrated that A- and C- site metal ion binding is affected as a direct result of the substitution of the pro-S_p oxygen atom of dATP with a sulfur atom. As the atom at the S_p position is expected to coordinate M_C, the larger atomic radius of sulfur relative to oxygen disrupts the binding and therefore likely explains the observed rate reduction *in crystallo*. In fact, M_C is not observed at all despite product formation (50% product at 600 s), which suggests that M_C may not be absolutely essential for catalysis. However, the authors argue that M_C must be present but is too transient or low occupancy to be observed in the electron density.[39] In addition, mutation of active site residue (R61) of hPolη to alanine, resulted in delayed third divalent metal ion binding and misalignment of the bound dNTP relative to the primer 3′-OH. This is somewhat unexpected considering that R61 in the pre-catalytic ternary crystal structures occupies the space where M_C would bind following catalytic metal ion exchange. Based on this single pre-catalytic rotameric

conformation, we expect that the exchange between pre- and post-catalytic side chain configurations of R61 is slow and may partially limit the rate of M_C binding. Therefore, it is reasonable to hypothesize that mutation of R61 to alanine would facilitate more efficient binding of M_C. However, considering that R61 makes important contacts with both the α- and β-phosphates of the incoming dNTP, and the primer 3′-OH is misaligned relative to wild-type structures, their results may simply reflect the negative impact of the mutation on nucleotide binding as suggested by the significant increase (~2-10-fold) in K_m compared to the wild-type enzyme in steady-state kinetic experiments.[80]

Altogether, the authors use these data to suggest that chemistry (Step 6, Scheme 1A) is indeed rate-limiting for hPolη, which contrasts with previous kinetic evidence,[103,104] and that M_C binding may provide the free energy needed to overcome the activation energy barrier for nucleotidyltransfer (*i.e.* transition-state stabilization). However, it is important to consider that hPolη is first crystallized in a ternary complex in the presence of non-catalytic Ca^{2+} and therefore only the bond forming chemistry step is observed. Substrate binding (Step 3, Scheme 1A) and any associated conformational rate-limiting steps (Steps 4 and 5, Scheme 1A) have presumably already occurred. Thus, the reduction in reaction rate caused by the postponement or disruption to third divalent metal ion binding caused by the S_p-dATPαS or R61A mutation suggest that M_C binding limits the rate of the chemistry step, but likely is not rate-limiting for the entire kinetic pathway for single-nucleotide incorporation (Scheme 1A, see Section 3.4). Altogether, this work confirmed and measured the binding of M_C to hPolη at reasonable metal ion concentrations (in contrast to work with hPolβ, 200 mM Mg^{2+}/Mn^{2+})[40-42,45] and correlates the M_C binding affinities estimated crystallographically and in-solution. However, this study falls short of unequivocally limiting the role of M_C to transition-state stabilization, as the temporal resolution afforded by the time-resolved crystallography technique[225] is not sufficient to distinguish the order of M_C binding and nucleotidyltransfer.

4.4 Evidence and hypothesized roles for the third divalent metal ion in single-nucleotide incorporation catalyzed by hPol*β*

Following the seminal study with hPol*η*,[38] time-resolved crystallography was employed to visualize nucleotide incorporation by hPol*β* on a gapped DNA substrate.[40] Interestingly, a third divalent metal ion at the C-site was also observed for hPol*β*[40] during correct nucleotide incorporation in a similar position to the third divalent metal ion in hPol*η* (Figure 3).[38] However, in contrast to the results obtained for hPol*η*,[38] M_C only appeared in the product complex structures and coincided with the loss of M_A. This observation suggested that M_C is solely involved in post-chemistry events and perhaps the diverse polymerase families utilize the third divalent metal ion in distinct ways. In fact, the timing of M_C binding suggested a role for M_C in pyrophosphorolysis, wherein it would stabilize the attacking oxygen atom of PP_i following proton abstraction by a water molecule (Figure 1C). Consistent with this hypothesis, open nicked DNA binary complex (E•DNA) crystals soaked with Mg^{2+} and PP_i yielded structures of the polymerase in the closed conformation with M_C and PP_i bound to the active site (*i.e.* reactant-state for reverse reaction, pyrophosphorolysis). However, these complexes failed to initiate pyrophosphorolysis, presumably because M_A was a Na^+ ion rather than the catalytic Mg^{2+}. Interestingly, M_C was not observed during incorrect nucleotide incorporation.[40]

The role of M_C in pyrophosphorolysis was further investigated through use of quantum mechanical/molecular mechanical computational methods.[50] It was determined that M_C was beneficial in the initial stages of the chemical reaction (*i.e.* initiating the attack of P*α* by O*β*), but became inhibitory as the two reacting atoms (P*α* and O*β*) approached a distance of 2.3 Å, likely due to the strict coordination distances and geometry of M_C, thus effectively preventing the transition-state from forming.[50] However, replacement of Mg^{2+} with Na^+ at the C-site resulted in a lowered activation energy barrier, suggesting a mechanism where metal ions may exchange during the reaction pathway to favor reaction completion.

In addition, the authors demonstrated that Mg^{2+} binding at the A-site is required for catalysis in either the forward or reverse (*i.e.* nucleotidyltransfer or pyrophosphorolysis) direction and rapid exchange with Na^{+} following catalysis effectively pushes the reaction to completion. The inability for Mg^{2+} at the C-site to support the reverse reaction but the requirement of Mg^{2+} at the A-site for forward and reverse catalysis is consistent with the hypothesis that M_C may only be involved in post-chemistry events (*i.e.* PP_i release or conformational changes) for hPol*β* and explains the inability of PP_i to support pyrophosphorolysis *in crystallo*.[43,50]

In subsequent time-resolved crystallographic investigations of hPol*β* during faithful and unfaithful translesion DNA synthesis across from the major oxidative lesion 8-oxo-7,8-dihydro-2′-deoxyguanine (8-oxoG) (Figure 7),[42] M_C was observed in the reaction-state (Figure 8A and B) and post-chemistry (Figure 8C and D) structures with its occupancy similar or equivalent to the product-state occupancy. Notably, as the reaction progressed, M_C moved towards its final position wherein it was fully coordinated with the reaction products and water molecules during bypass of 8-oxoG with dATP, highlighting the dynamic nature of the third divalent metal ion. This observation is similar to hPol*η* wherein M_C binding occurs prior to or immediately following reaction initiation,[38,39] and suggests that M_C may diffuse into the hPol*β* active site following reaction initiation to associate with reaction intermediates as a means to stabilize the transition-state. This result was further supported in a follow-up time-resolved crystallographic study following hPol*β*-catalyzed extension from 8-oxoG containing base pairs which were generated during the bypass[45] (*i.e.* dC:8-oxoG or dA:8-oxoG was the primer-template junction pair). Importantly, during this study,[45] M_C was observed as early as 15% product formation, suggesting an early role in catalysis (*i.e.* transition-state stabilization). Furthermore, the investigation of post-chemistry events for hPol*β*-catalyzed nucleotide incorporation, revealed that M_C is not involved in PP_i release (see Section 3.5), thus limiting the third divalent metal ion to function in chemical events

such as transition-state stabilization or product-state stabilization.

Additional time-resolved studies following the incorporation of 8-oxo-dGTP opposite a template dC or dA[41] or the extension from these incorporation products (*i.e.* 8-oxoG:dC or 8-oxoG:dA were the primer-template junction pair)[44] similarly demonstrated that M_C appears in reaction- and product-state structures. Unexpectedly, the third divalent metal ion appeared in the pre-catalytic structure for incorporation of 8-oxo-dGTP opposite dC presumably as a result of favorable M_C coordination facilitated by the optimal position of the O8 modification of the damaged nucleotide. The inclusion of a third coordinating ligand offered by the O8 atom, in addition to the non-bridging oxygen atoms on the α- and β-phosphates, likely makes M_C binding more favorable in this structure.[41] These damage-specific interactions coupled with the absence of M_C in all other pre-catalytic structures from time-resolved crystallographic investigations of hPolβ suggest that pre-catalytic M_C binding is likely unique to this damage DNA context and therefore does not represent a common mechanistic feature. Nevertheless, despite the appearance of M_C in reaction intermediate structures, the authors argue that the third divalent metal ion is only involved in post-chemistry events and does not provide transition-state stabilization.[41,44]

To further investigate the role of M_C in the forward nucleotidyltransfer reaction a similar computational investigation as that completed for hPolβ-catalyzed pyrophosphorolysis[50] was performed.[51] As coordination of M_C by the bridging oxygen (O$\alpha\beta$) between the Pα and Pβ of the incoming nucleotide can only occur after the phosphodiester bond (*i.e.* Pα–O$\alpha\beta$) is broken, molecular dynamics was used to determine the position of the Mg^{2+} prior to nucleotidyltransfer. The calculated position of modeled pre-catalytic M_C was similar to that experimentally observed for M_C. However, the modeled pre-catalytic M_C is coordinated by the Pα pro-S_p oxygen of the incoming nucleotide and five water molecules, rather than the experimentally observed coordination by the Pα pro-S_p oxygen of the

incorporated nucleotide, O$\alpha\beta$ of PP_i, and four water molecules. Within this system, the simulated activation energy barrier for nucleotidyltransfer was calculated to be 16.6 to 18.1 kcal/mol and, except for a slight repositioning of the product PP_i, very few differences in active site structure were observed relative to the time-resolved studies.[40-42,44,45] Interestingly, a two Mg^{2+} system in which M_C was omitted and only M_A and M_B were used gave a very similar activation energy barrier of 17.5 to 18.6 kcal/mol, suggesting that M_C does not appreciably aid nucleotidyltransfer. Consistent with these computational predictions, the incorporation of a phosphorothioate nucleotide analog, S_p-dCTPαS, in which the sulfur substitution should ablate M_C binding, was only 3-fold slower than incorporation of dCTP.[146] Moreover, time-resolved crystallography of dCTPαS incorporation did not reveal the presence of a third divalent metal ion following nucleotide incorporation.[51] Taken together, these evidences suggest that the third divalent metal ion does not aid the forward reaction by significantly lowering the activation barrier,[50,51] which is in contrast to hPolη.[39] Alternatively, in a two Mg^{2+} (M_A and M_B) and one Na^+ (M_C) system the activation energy barrier is significantly lowered to 11.6 to 13.2 kcal/mol, suggesting a possible mechanism wherein a Na^+ is initially bound at the C-site to assist nucleotidyltransfer and is subsequently exchanged with Mg^{2+} following incorporation in order to prevent pyrophosphorolysis. This hypothesized metal ion exchange at the C-site is akin to the structurally observed exchange of the A-site Mg^{2+} for Na^+ following nucleotidyltransfer,[40-42,44,45] which also prevents pyrophosphorolysis. These metal ion exchanges within the hPolβ active site may act to favor nucleotidyltransfer while disfavoring pyrophosphorolysis.

While the first time-resolved structural study of hPolβ documenting a third divalent metal ion showed the appearance of M_C only after full product formation,[40] the latter four investigations showed M_C binding coinciding exactly with product formation,[41,42,44,45] which is consistent with the reports of the third divalent metal ion for hPolη.[38,39] Accordingly, it is unclear for hPolβ if M_C binds prior to and

supports nucleotidyltransfer, or binds following nucleotidyltransfer to stabilize the product complex (*i.e.* preventing pyrophosphorolysis).[50] Altogether, conflicting results from the time-resolved[40-42,44,45] and computational studies,[50,51] as well as the aforementioned investigation of hPolβ post-chemistry events[43] (see Section 3.5) limits the potential roles of M_C to either transition-state stabilization during nucleotidyltransfer (Figure 1B) or suppression of pyrophosphorolysis through stabilization of the product complex. However, similar concentration dependent divalent metal ion soaks to those with hPolη[39] to determine the effect of M_C on enzymatic rate are necessary to experimentally demonstrate whether or not M_C aids nucleotidyltransfer through transition-state stabilization.

4.5. Evidence and hypothesized roles for the third divalent metal ion in single-nucleotide incorporation catalyzed by hPolμ

Similar to studies with hPolβ,[40-45] time-resolved crystallography was used to follow nucleotide incorporation into single-nucleotide gapped DNA by hPolμ,[46] wherein the pre-catalytic ternary complex formed in the presence of non-catalytic Ca^{2+} was soaked with either Mg^{2+} or Mn^{2+} to initiate metal ion exchange and catalysis. In contrast to the time-resolved structural findings with hPolβ[40-42,44,45] and hPolη,[38,39] a third divalent metal ion bound at the C-site could not be observed with Mg^{2+} even after extensive soaking at a high concentration of Mg^{2+} (100 mM) and despite full product formation. As expected, the Mg^{2+} bound at the A-site was eventually replaced by Na^+ at longer time points showing complete product formation. On the other hand, soaking with Mn^{2+} resulted in appearance of M_C at time points coincident with 40% product formation and beyond, as well as sustained presence of Mn^{2+} at the A- and B-sites at every time point therefore suggesting that Mn^{2+} may be the physiological catalytic divalent metal ion for hPolμ and perhaps other DNA polymerases that exhibit low activity with Mg^{2+}. Notably, the position of M_C and the coordination of M_C by the reaction products, as well as the timing of

M_C, are consistent with that observed for hPolβ[40-45] and hPolη.[38,39] Based on the computational work with hPolβ,[50,51] occupancy of the A-site by a divalent metal ion is essential for pyrophosphorolysis whereas the presence of M_C is inhibitory (see Section 4.4). As hPolβ and hPolμ share significant structural similarity, the roles of M_A and M_C for the reverse reaction may be conserved between these two polymerases. Accordingly, by analogy to hPolβ (see Section 4.4), the A-site metal ion exchange to Na^+ in the presence of Mg^{2+} observed with hPolμ likely precludes pyrophosphorolysis and therefore a third divalent metal ion may not be necessary to suppress this reaction when Mg^{2+} is supplied as the catalytic metal ion. However, the persistence of M_A in the presence of Mn^{2+} necessitates binding of M_C to prevent pyrophosphorolysis.

Single-nucleotide incorporation experiments with S_p-dTTPαS (see Section 3.4.1) suggest that M_C could serve a role in nucleotidyltransfer as experiments in the presence of Mg^{2+}, wherein M_C should not be bound, demonstrated a strong elemental effect, whereas this effect was lost in the presence of Mn^{2+} and presumably M_C.[46] However, in their publication, the authors suggest that absence of an elemental effect with Mn^{2+} was not due to binding of M_C as i) C-site divalent metal ion binding occurred following nucleotidyltransfer in the time-dependent structures (*i.e.* occupancy corresponded exactly with product accumulation), ii) Mn^{2+} is generally considered thio-phobic,[232] and iii) the sulfur substitution of the pro-S_p oxygen would likely disrupt M_C coordination. Thus, similar to their work with hPolβ (see Section 4.4),[51] the authors suggest that M_C is not involved in transition-state stabilization during nucleotidyltransfer but rather serves to stabilize the product state to prevent pyrophosphorolysis. Nevertheless, the simultaneous appearance of M_C and reaction products could just as easily imply that the third divalent metal ion is critical for nucleotidyltransfer. Moreover, the expected disruption of M_C binding by the longer P–S bond distance would likely be alleviated by the flexibility of the other coordinating ligands, as four of six are water molecules. Fittingly, it is possible that M_C provides the

necessary transition-state stabilization to accelerate the chemistry step in the presence of Mn^{2+} thereby eliminating the elemental effect. In this scenario, the results would be consistent with those of hPolη (see Section 4.3).[39]

Similar to our recent investigation of hPolβ-catalyzed post-chemistry events,[43] during time-dependent crystallography of hPolμ, M_C was also observed to dissociate before PP_i.[46] While hPolβ displays a large open→closed conformational change of the thumb domain (Figure 2) during nucleotide binding (see Section 3.4), such a large change is not observed for hPolμ, which may explain why time-resolved structural capture of the order of M_C and PP_i dissociation was difficult for hPolβ (*i.e.* rapid domain motion of hPolβ results in loss of synchronization of *in crystallo* events and associated electron density, see Section 3.5), but readily possible for hPolμ. Altogether, the time-resolved structural study of hPolμ,[46] featuring the third divalent metal ion, parallel those of hPolβ[40-45] and suggest a conserved role for M_C during X-family polymerase-catalyzed DNA synthesis. However, more work is needed to explicitly delineate the mechanistic function of M_C in transition-state stabilization or preventing pyrophosphorolysis.

4.6. Future characterization of the third divalent metal ion

The role of M_C in single-nucleotide incorporation is not well-defined with compelling evidence to support its involvement in i) stabilizing the transition-state of nucleotidyltransfer, ii) supporting pyrophosphate release, and/or iii) promoting or suppressing pyrophosphorolysis. It is clear from the limited work investigating the third divalent metal ion that its function in DNA polymerase catalysis is complex and may differ between the X- and Y-family polymerases. For example, the complementary time-resolved crystallographic[40-45] and computational studies[50,51] completed for hPolβ (see Section 4.4) support the proposed roles of M_C and provide an argument for analogous functions in hPolμ (see Section

4.5).[46] However, a potential role in transition-state stabilization for M_C in the X-family DNA polymerases cannot be completely ruled out. Conversely, for hPolη, it has been proposed that M_C is directly involved in transition-state stabilization during nucleotide incorporation.[39,198] Nevertheless, additional work must be completed with other Y-family polymerases to validate the proposed roles of M_C suggested for hPolη (see Section 4.3) and to determine if M_C function is conserved for the Y-family polymerases. In addition, computational investigations, such as those performed for hPolβ,[50,51] must be undertaken for hPolμ and hPolη to better substantiate the proposed roles of M_C in these polymerases. Similarly, concentration dependent metal ion soaking as performed for hPolη[39] must be performed for hPolβ and hPolμ to determine if M_C also acts in transition-state stabilization for these polymerases as argued for hPolη,[39,198] especially considering that high metal ion concentrations of ~200 mM were used for the studies of hPolβ[40-45] and could negatively affect polymerase activity.[93,109,233,234]

Furthermore, the apparent differences between how M_C is utilized between the X- and Y-family polymerases advocates for future research on the A- or B-family replicative polymerases as well as RTs to determine if a third divalent metal ion is used at all, and if so, what apparent role does it serve, and how does this compare to results of hPolη,[38,39] hPolβ,[40-45] and hPolμ.[46] Importantly, if a third divalent metal ion is observed for viral DNA polymerases or RTs and serves a purpose in catalysis (*i.e.* transition-state stabilization as with hPolη), then it may be a potential therapeutic target. For example, the active site of HIV-1 RT is very comparable to that of hPolη and contains an equivalent arginine residue (see Section 4.3) that may function similarly with the third divalent metal ion to facilitate nucleotidyltransfer and pyrophosphorolysis (Figure 3). As HIV-1 RT is known to remove chain-terminating nucleotide analogs by pyrophosphorolysis,[235] design of antiviral small molecules to specifically block the third divalent metal ion binding may prove to be an effective treatment strategy. Finally, as it stands, the only experimental evidence for the third divalent metal ion comes from X-ray

structures capturing *in crystallo* reaction progression. Accordingly, it is possible that these findings may represent an artifact of the structural technique. Therefore, we expect that advanced spectroscopic methods such as electroparamagnetic resonance (EPR) spectroscopy,[236] will be necessary to fully validate and further elucidate the function of the third divalent metal ion during polymerase catalysis under a more physiological context.

5. Concluding Remarks

Despite thousands of published studies investigating the structure and mechanism of DNA polymerases and RTs, it is abundantly clear that there is so much more to learn. Indeed, as the kinetics and conformational dynamics of each step of the DNA synthesis mechanism have been rigorously investigated for many polymerases from all of the diverse families, it is becoming evident that a singular, unified mechanism to describe every unique aspect of polymerase catalysis, including polymerase fidelity, is unrealistic. Thus far, it is evident that conformational dynamics differentially impact various aspects of the catalytic and kinetic mechanism between DNA polymerase and RT families, or even within a family. In the coming years, research to better understand the contributions of polymerase conformational dynamics during DNA binding and translocation, nucleotide binding, selectivity, and incorporation, pyrophosphate binding, and pyrophosphorolysis to the mechanism of DNA polymerization will be paramount.

The skillful application of time-resolved X-ray crystallography to study DNA polymerases has enabled the discovery of a third divalent metal ion during single-nucleotide incorporation. Remarkably, this third divalent metal ion may be important for DNA polymerase and RT catalysis which shifts the long-standing paradigm of two-metal-ion catalysis for DNA polymerization. We are excited at the prospect of identifying the third divalent metal ion in other families of DNA polymerases and RTs to

determine if a three-metal-ion mechanism is conserved for DNA synthesis. To date, the third divalent metal ion has only been captured in two X-family members and one Y-family member, but the significant differences in the proposed function of the third divalent metal ion, already apparent between these two families, implore future research of other polymerase families in hopes of exploiting potential drug targets for developing novel antiviral and antibiotic small molecule therapeutics.

6. Author Information

6.1. Corresponding Author

*E-mail: suo.3@osu.edu

6.2. Notes

The authors declare no competing financial interest.

6.3. Biographies

Austin T. Raper graduated *Summa Cum Laude* from the University of Mount Union in 2013 with a B.S. in Biochemistry. As a 2017-2018 Presidential Fellow of The Ohio State University and member of the Ohio State Biochemistry Program, he is conducting his dissertation research in the laboratory of Dr. Zucai Suo (Department of Chemistry and Biochemistry) to earn a Ph.D. in Biochemistry. A.T.R. is also a former fellow of the Chemistry and Biology Interface Training Program at The Ohio State University. His research focus is on characterizing enzymes critical for DNA lesion bypass and repair as well as gene-editing using pre-steady-state kinetics and single-molecule enzymology.

Andrew J. Reed received his B.S. in Biochemistry from the University of Mount Union in 2013. As a

member of the Ohio State Biochemistry Program and the Pelotonia Fellowship Program, he is currently researching in the laboratory of Dr. Zucai Suo (Department of Chemistry and Biochemistry) at The Ohio State University in pursuit of a Ph.D. in Biochemistry. Andrew is investigating enzymes critical for DNA replication, base excision repair, and lesion bypass through X-ray crystallographic and pre-steady-state kinetic techniques.

Zucai Suo received both B.S. in chemistry and M.S. in physical chemistry from Fudan University in China and his Ph.D. in chemistry in the laboratory of Kenneth A. Johnson at Pennsylvania State University. He was then a Jane Coffin Childs Memorial Fund Postdoctoral Fellow for two years at Harvard Medical School in the laboratory of Christopher T. Walsh. Subsequently, he worked as a senior biochemist at Eli Lilly. Since October 2001, Dr. Suo has been a professor at The Ohio State University. He was elected to be a fellow of the American Association for the Advancement of Science and has served in different administrative roles for the Division of Chemical Toxicology of the American Chemical Society. His research interests include kinetic, dynamic, and structure-function relationship studies of DNA polymerases and gene-editing enzymes as well as antiviral and anticancer drug discovery.

7. Acknowledgements

This work was financially supported by the National Science Foundation grant MCB-1716168 to Z.S. A.T.R and A.J.R were respectively supported by a Presidential Fellowship and a Pelotonia Fellowship from The Ohio State University. Any opinions, findings, and conclusions expressed in this material are those of the author(s) and do not necessarily reflect those of the Pelotonia Fellowship Program.

8. References

(1) Palermo, G.; Cavalli, A.; Klein, M. L.; Alfonso-Prieto, M.; Dal Peraro, M.; De Vivo, M. Catalytic Metal Ions and Enzymatic Processing of DNA and RNA. *Acc. Chem. Res.* **2015,** *48*, 220-228.

(2) Yang, W.; Lee, J. Y.; Nowotny, M. Making and Breaking Nucleic Acids: Two-Mg^{2+}-Ion Catalysis and Substrate Specificity. *Mol. Cell* **2006,** *22*, 5-13.

(3) Steitz, T. A.; Steitz, J. A. A General Two-Metal-Ion Mechanism for Catalytic RNA. *Proc. Natl. Acad. Sci. U. S. A.* **1993,** *90*, 6498-6502.

(4) Johnson, K. A. Conformational Coupling in DNA Polymerase Fidelity. *Annu. Rev. Biochem.* **1993,** *62*, 685-713.

(5) Joyce, C. M.; Benkovic, S. J. DNA Polymerase Fidelity: Kinetics, Structure, and Checkpoints. *Biochemistry* **2004,** *43*, 14317-14324.

(6) Showalter, A. K.; Tsai, M. D. A Reexamination of the Nucleotide Incorporation Fidelity of DNA Polymerases. *Biochemistry* **2002,** *41*, 10571-10576.

(7) Rothwell, P. J.; Mitaksov, V.; Waksman, G. Motions of the Fingers Subdomain of Klentaq1 Are Fast and Not Rate Limiting: Implications for the Molecular Basis of Fidelity in DNA Polymerases. *Mol. Cell* **2005,** *19*, 345-355.

(8) Rothwell, P. J.; Waksman, G. Structure and Mechanism of DNA Polymerases. *Adv. Protein Chem.* **2005,** *71*, 401-440.

(9) Raper, A. T.; Gadkari, V. V.; Maxwell, B. A.; Suo, Z. Single-Molecule Investigation of Response to Oxidative DNA Damage by a Y-Family DNA Polymerase. *Biochemistry* **2016,** *55*, 2187-2196.

(10) Raper, A. T.; Suo, Z. Investigation of Intradomain Motions of a Y-Family DNA Polymerase During Substrate Binding and Catalysis. *Biochemistry* **2016,** *55*, 5832-5844.

(11) Xu, C.; Maxwell, B. A.; Brown, J. A.; Zhang, L.; Suo, Z. Global Conformational Dynamics of a Y-Family DNA Polymerase During Catalysis. *PLoS Biol.* **2009,** *7*, e1000225.

(12) Maxwell, B. A.; Xu, C.; Suo, Z. DNA Lesion Alters Global Conformational Dynamics of Y-Family DNA Polymerase During Catalysis. *J. Biol. Chem.* **2012,** *287*, 13040-13047.

(13) Maxwell, B. A.; Xu, C.; Suo, Z. Conformational Dynamics of a Y-Family DNA Polymerase During Substrate Binding and Catalysis as Revealed by Interdomain Forster Resonance Energy Transfer. *Biochemistry* **2014,** *53*, 1768-1778.

(14) Xu, C.; Maxwell, B. A.; Suo, Z. Conformational Dynamics of *Thermus aquaticus* DNA Polymerase I During Catalysis. *J. Mol. Biol.* **2014,** *426*, 2901-2917.

(15) Bessman, M. J.; Kornberg, A.; Lehman, I. R.; Simms, E. S. Enzymic Synthesis of Deoxyribonucleic Acid. *Biochim. Biophys. Acta* **1956,** *21*, 197-198.

(16) Lehman, I. R.; Bessman, M. J.; Simms, E. S.; Kornberg, A. Enzymatic Synthesis of Deoxyribonucleic Acid. I. Preparation of Substrates and Partial Purification of an Enzyme from *Escherichia coli*. *J. Biol. Chem.* **1958,** *233*, 163-170.

(17) Joyce, C. M.; Steitz, T. A. Function and Structure Relationships in DNA Polymerases. *Annu. Rev. Biochem.* **1994,** *63*, 777-822.

(18) Braithwaite, D. K.; Ito, J. Compilation, Alignment, and Phylogenetic Relationships of DNA Polymerases. *Nucleic Acids Res.* **1993,** *21*, 787-802.

(19) Garcia-Diaz, M.; Bebenek, K. Multiple Functions of DNA Polymerases. *CRC Crit. Rev. Plant Sci.* **2007,** *26*, 105-122.

(20) Yang, W.; Gao, Y. Translesion and Repair DNA Polymerases: Diverse Structure and Mechanism. *Annu. Rev. Biochem.* **2018**.
(21) Beard, W. A.; Wilson, S. H. Structure and Mechanism of DNA Polymerase Beta. *Biochemistry* **2014,** *53*, 2768-2780.
(22) Maxwell, B. A.; Suo, Z. Recent Insight into the Kinetic Mechanisms and Conformational Dynamics of Y-Family DNA Polymerases. *Biochemistry* **2014,** *53*, 2804-2814.
(23) Fowler, J. D.; Suo, Z. Biochemical, Structural, and Physiological Characterization of Terminal Deoxynucleotidyl Transferase. *Chem. Rev.* **2006,** *106*, 2092-2110.
(24) Berdis, A. J. Mechanisms of DNA Polymerases. *Chem. Rev.* **2009,** *109*, 2862-2879.
(25) Steitz, T. A. DNA Polymerases: Structural Diversity and Common Mechanisms. *J. Biol. Chem.* **1999,** *274*, 17395-17398.
(26) Steitz, T. A. A Mechanism for All Polymerases. *Nature* **1998,** *391*, 231-232.
(27) Tsai, Y. C.; Johnson, K. A. A New Paradigm for DNA Polymerase Specificity. *Biochemistry* **2006,** *45*, 9675-9687.
(28) Xiang, Y.; Goodman, M. F.; Beard, W. A.; Wilson, S. H.; Warshel, A. Exploring the Role of Large Conformational Changes in the Fidelity of DNA Polymerase Beta. *Proteins* **2008,** *70*, 231-247.
(29) Wong, I.; Patel, S. S.; Johnson, K. A. An Induced-Fit Kinetic Mechanism for DNA Replication Fidelity: Direct Measurement by Single-Turnover Kinetics. *Biochemistry* **1991,** *30*, 526-537.
(30) Freemont, P. S.; Friedman, J. M.; Beese, L. S.; Sanderson, M. R.; Steitz, T. A. Cocrystal Structure of an Editing Complex of Klenow Fragment with DNA. *Proc. Natl. Acad. Sci. U. S. A.* **1988,** *85*, 8924-8928.
(31) Beese, L. S.; Steitz, T. A. Structural Basis for the 3'-5' Exonuclease Activity of *Escherichia coli* DNA Polymerase I: A Two Metal Ion Mechanism. *EMBO J.* **1991,** *10*, 25-33.
(32) Batra, V. K.; Beard, W. A.; Shock, D. D.; Krahn, J. M.; Pedersen, L. C.; Wilson, S. H. Magnesium-Induced Assembly of a Complete DNA Polymerase Catalytic Complex. *Structure* **2006,** *14*, 757-766.
(33) Brautigam, C. A.; Steitz, T. A. Structural and Functional Insights Provided by Crystal Structures of DNA Polymerases and Their Substrate Complexes. *Curr. Opin. Struct. Biol.* **1998,** *8*, 54-63.
(34) Nakamura, T. Z., Ye; Yamagata, Yuriko; Hua, Yue-jin; Yang, Wei;. Mechanism of the Nucleotidyl-Transfer Reaction in DNA Polymerase Revealed by Time-Resolved Crystallography. *Biophysics* **2013,** *9*, 31-36.
(35) Yang, W. Damage Repair DNA Polymerases Y. *Curr. Opin. Struct. Biol.* **2003,** *13*, 23-30.
(36) Yang, W. An Equivalent Metal Ion in One- and Two-Metal-Ion Catalysis. *Nat. Struct. Mol. Biol.* **2008,** *15*, 1228-1231.
(37) Derbyshire, V.; Freemont, P. S.; Sanderson, M. R.; Beese, L.; Friedman, J. M.; Joyce, C. M.; Steitz, T. A. Genetic and Crystallographic Studies of the 3',5'-Exonucleolytic Site of DNA Polymerase I. *Science* **1988,** *240*, 199-201.
(38) Nakamura, T.; Zhao, Y.; Yamagata, Y.; Hua, Y. J.; Yang, W. Watching DNA Polymerase Eta Make a Phosphodiester Bond. *Nature* **2012,** *487*, 196-201.
(39) Gao, Y.; Yang, W. Capture of a Third Mg(2)(+) Is Essential for Catalyzing DNA Synthesis. *Science* **2016,** *352*, 1334-1337.
(40) Freudenthal, B. D.; Beard, W. A.; Shock, D. D.; Wilson, S. H. Observing a DNA Polymerase Choose Right from Wrong. *Cell* **2013,** *154*, 157-168.

(41) Freudenthal, B. D.; Beard, W. A.; Perera, L.; Shock, D. D.; Kim, T.; Schlick, T.; Wilson, S. H. Uncovering the Polymerase-Induced Cytotoxicity of an Oxidized Nucleotide. *Nature* **2015,** *517*, 635-639.
(42) Vyas, R.; Reed, A. J.; Tokarsky, E. J.; Suo, Z. Viewing Human DNA Polymerase Beta Faithfully and Unfaithfully Bypass an Oxidative Lesion by Time-Dependent Crystallography. *J. Am. Chem. Soc.* **2015,** *137*, 5225-5230.
(43) Reed, A. J.; Vyas, R.; Raper, A. T.; Suo, Z. Structural Insights into the Post-Chemistry Steps of Nucleotide Incorporation Catalyzed by a DNA Polymerase. *J. Am. Chem. Soc.* **2017,** *139*, 465-471.
(44) Whitaker, A. M.; Smith, M. R.; Schaich, M. A.; Freudenthal, B. D. Capturing a Mammalian DNA Polymerase Extending from an Oxidized Nucleotide. *Nucleic Acids Res.* **2017,** *45*, 6934-6944.
(45) Reed, A. J.; Suo, Z. Time-Dependent Extension from an 8-Oxoguanine Lesion by Human DNA Polymerase Beta. *J. Am. Chem. Soc.* **2017,** *139*, 9684-9690.
(46) Jamsen, J. A.; Beard, W. A.; Pedersen, L. C.; Shock, D. D.; Moon, A. F.; Krahn, J. M.; Bebenek, K.; Kunkel, T. A.; Wilson, S. H. Time-Lapse Crystallography Snapshots of a Double-Strand Break Repair Polymerase in Action. *Nat. Commun.* **2017,** *8*, 253.
(47) Yang, W.; Weng, P. J.; Gao, Y. A New Paradigm of DNA Synthesis: Three-Metal-Ion Catalysis. *Cell Biosci* **2016,** *6*, 51.
(48) Freudenthal, B. D.; Beard, W. A.; Wilson, S. H. New Structural Snapshots Provide Molecular Insights into the Mechanism of High Fidelity DNA Synthesis. *DNA Repair (Amst)* **2015,** *32*, 3-9.
(49) Genna, V.; Gaspari, R.; Dal Peraro, M.; De Vivo, M. Cooperative Motion of a Key Positively Charged Residue and Metal Ions for DNA Replication Catalyzed by Human DNA Polymerase-Eta. *Nucleic Acids Res.* **2016,** *44*, 2827-2836.
(50) Perera, L.; Freudenthal, B. D.; Beard, W. A.; Shock, D. D.; Pedersen, L. G.; Wilson, S. H. Requirement for Transient Metal Ions Revealed through Computational Analysis for DNA Polymerase Going in Reverse. *Proc. Natl. Acad. Sci. U. S. A.* **2015,** *112*, E5228-5236.
(51) Perera, L.; Freudenthal, B. D.; Beard, W. A.; Pedersen, L. G.; Wilson, S. H. Revealing the Role of the Product Metal in DNA Polymerase Beta Catalysis. *Nucleic Acids Res.* **2017,** *45*, 2736-2745.
(52) Liu, X.; Bushnell, D. A.; Kornberg, R. D. RNA Polymerase II Transcription: Structure and Mechanism. *Biochim. Biophys. Acta* **2013,** *1829*, 2-8.
(53) Svetlov, V.; Nudler, E. Basic Mechanism of Transcription by RNA Polymerase II. *Biochim. Biophys. Acta* **2013,** *1829*, 20-28.
(54) Hahn, S. Structure and Mechanism of the RNA Polymerase II Transcription Machinery. *Nat. Struct. Mol. Biol.* **2004,** *11*, 394-403.
(55) Kochetkov, S. N.; Rusakova, E. E.; Tunitskaya, V. L. Recent Studies of T7 RNA Polymerase Mechanism. *FEBS Lett.* **1998,** *440*, 264-267.
(56) Ebright, R. H. RNA Polymerase: Structural Similarities between Bacterial RNA Polymerase and Eukaryotic RNA Polymerase II. *J. Mol. Biol.* **2000,** *304*, 687-698.
(57) Moon, A. F.; Garcia-Diaz, M.; Batra, V. K.; Beard, W. A.; Bebenek, K.; Kunkel, T. A.; Wilson, S. H.; Pedersen, L. C. The X Family Portrait: Structural Insights into Biological Functions of X Family Polymerases. *DNA Repair (Amst)* **2007,** *6*, 1709-1725.
(58) Burgers, P. M. J.; Kunkel, T. A. Eukaryotic DNA Replication Fork. *Annu. Rev. Biochem.* **2017,** *86*, 417-438.

(59) Kohlstaedt, L. A.; Wang, J.; Friedman, J. M.; Rice, P. A.; Steitz, T. A. Crystal Structure at 3.5 a Resolution of HIV-1 Reverse Transcriptase Complexed with an Inhibitor. *Science* **1992,** *256*, 1783-1790.
(60) Steitz, T. A.; Smerdon, S.; Jager, J.; Wang, J.; Kohlstaedt, L. A.; Friedman, J. M.; Beese, L. S.; Rice, P. A. Two DNA Polymerases: HIV Reverse Transcriptase and the Klenow Fragment of *Escherichia coli* DNA Polymerase I. *Cold Spring Harb. Symp. Quant. Biol.* **1993,** *58*, 495-504.
(61) Pelletier, H.; Sawaya, M. R.; Kumar, A.; Wilson, S. H.; Kraut, J. Structures of Ternary Complexes of Rat DNA Polymerase Beta, a DNA Template-Primer, and Ddctp. *Science* **1994,** *264*, 1891-1903.
(62) Sawaya, M. R.; Pelletier, H.; Kumar, A.; Wilson, S. H.; Kraut, J. Crystal Structure of Rat DNA Polymerase Beta: Evidence for a Common Polymerase Mechanism. *Science* **1994,** *264*, 1930-1935.
(63) Doublie, S.; Tabor, S.; Long, A. M.; Richardson, C. C.; Ellenberger, T. Crystal Structure of a Bacteriophage T7 DNA Replication Complex at 2.2 a Resolution. *Nature* **1998,** *391*, 251-258.
(64) Li, Y.; Kong, Y.; Korolev, S.; Waksman, G. Crystal Structures of the Klenow Fragment of *Thermus aquaticus* DNA Polymerase I Complexed with Deoxyribonucleoside Triphosphates. *Protein Sci.* **1998,** *7*, 1116-1123.
(65) Li, Y.; Korolev, S.; Waksman, G. Crystal Structures of Open and Closed Forms of Binary and Ternary Complexes of the Large Fragment of *Thermus aquaticus* DNA Polymerase I: Structural Basis for Nucleotide Incorporation. *EMBO J.* **1998,** *17*, 7514-7525.
(66) Korolev, S.; Nayal, M.; Barnes, W. M.; Di Cera, E.; Waksman, G. Crystal Structure of the Large Fragment of *Thermus aquaticus* DNA Polymerase I at 2.5-a Resolution: Structural Basis for Thermostability. *Proc. Natl. Acad. Sci. U. S. A.* **1995,** *92*, 9264-9268.
(67) Wang, J.; Yu, P.; Lin, T. C.; Konigsberg, W. H.; Steitz, T. A. Crystal Structures of an Nh2-Terminal Fragment of T4 DNA Polymerase and Its Complexes with Single-Stranded DNA and with Divalent Metal Ions. *Biochemistry* **1996,** *35*, 8110-8119.
(68) Franklin, M. C.; Wang, J.; Steitz, T. A. Structure of the Replicating Complex of a Pol Alpha Family DNA Polymerase. *Cell* **2001,** *105*, 657-667.
(69) Hogg, M.; Wallace, S. S.; Doublie, S. Crystallographic Snapshots of a Replicative DNA Polymerase Encountering an Abasic Site. *EMBO J.* **2004,** *23*, 1483-1493.
(70) Wang, M.; Xia, S.; Blaha, G.; Steitz, T. A.; Konigsberg, W. H.; Wang, J. Insights into Base Selectivity from the 1.8 a Resolution Structure of an Rb69 DNA Polymerase Ternary Complex. *Biochemistry* **2011,** *50*, 581-590.
(71) Evans, R. J.; Davies, D. R.; Bullard, J. M.; Christensen, J.; Green, L. S.; Guiles, J. W.; Pata, J. D.; Ribble, W. K.; Janjic, N.; Jarvis, T. C. Structure of Polc Reveals Unique DNA Binding and Fidelity Determinants. *Proc. Natl. Acad. Sci. U. S. A.* **2008,** *105*, 20695-20700.
(72) Bailey, S.; Wing, R. A.; Steitz, T. A. The Structure of *T. aquaticus* DNA Polymerase III Is Distinct from Eukaryotic Replicative DNA Polymerases. *Cell* **2006,** *126*, 893-904.
(73) Wing, R. A.; Bailey, S.; Steitz, T. A. Insights into the Replisome from the Structure of a Ternary Complex of the DNA Polymerase III Alpha-Subunit. *J. Mol. Biol.* **2008,** *382*, 859-869.
(74) Barros, T.; Guenther, J.; Kelch, B.; Anaya, J.; Prabhakar, A.; O'Donnell, M.; Kuriyan, J.; Lamers, M. H. A Structural Role for the Php Domain in *E. coli* DNA Polymerase III. *BMC Struct. Biol.* **2013,** *13*, 8.
(75) Pelletier, H.; Sawaya, M. R.; Wolfle, W.; Wilson, S. H.; Kraut, J. A Structural Basis for Metal Ion Mutagenicity and Nucleotide Selectivity in Human DNA Polymerase Beta. *Biochemistry* **1996,** *35*, 12762-12777.

(76) Garcia-Diaz, M.; Bebenek, K.; Krahn, J. M.; Kunkel, T. A.; Pedersen, L. C. A Closed Conformation for the Pol Lambda Catalytic Cycle. *Nat. Struct. Mol. Biol.* **2005,** *12*, 97-98.
(77) Moon, A. F.; Garcia-Diaz, M.; Bebenek, K.; Davis, B. J.; Zhong, X.; Ramsden, D. A.; Kunkel, T. A.; Pedersen, L. C. Structural Insight into the Substrate Specificity of DNA Polymerase Mu. *Nat. Struct. Mol. Biol.* **2007,** *14*, 45-53.
(78) Pelletier, H.; Sawaya, M. R.; Wolfle, W.; Wilson, S. H.; Kraut, J. Crystal Structures of Human DNA Polymerase Beta Complexed with DNA: Implications for Catalytic Mechanism, Processivity, and Fidelity. *Biochemistry* **1996,** *35*, 12742-12761.
(79) Sawaya, M. R.; Prasad, R.; Wilson, S. H.; Kraut, J.; Pelletier, H. Crystal Structures of Human DNA Polymerase Beta Complexed with Gapped and Nicked DNA: Evidence for an Induced Fit Mechanism. *Biochemistry* **1997,** *36*, 11205-11215.
(80) Biertumpfel, C.; Zhao, Y.; Kondo, Y.; Ramon-Maiques, S.; Gregory, M.; Lee, J. Y.; Masutani, C.; Lehmann, A. R.; Hanaoka, F.; Yang, W. Structure and Mechanism of Human DNA Polymerase Eta. *Nature* **2010,** *465*, 1044-1048.
(81) Irimia, A.; Eoff, R. L.; Guengerich, F. P.; Egli, M. Structural and Functional Elucidation of the Mechanism Promoting Error-Prone Synthesis by Human DNA Polymerase Kappa Opposite the 7,8-Dihydro-8-Oxo-2'-Deoxyguanosine Adduct. *J. Biol. Chem.* **2009,** *284*, 22467-22480.
(82) Nair, D. T.; Johnson, R. E.; Prakash, S.; Prakash, L.; Aggarwal, A. K. Replication by Human DNA Polymerase-Iota Occurs by Hoogsteen Base-Pairing. *Nature* **2004,** *430*, 377-380.
(83) Swan, M. K.; Johnson, R. E.; Prakash, L.; Prakash, S.; Aggarwal, A. K. Structure of the Human Rev1-DNA-dNTP Ternary Complex. *J. Mol. Biol.* **2009,** *390*, 699-709.
(84) Ling, H.; Boudsocq, F.; Woodgate, R.; Yang, W. Crystal Structure of a Y-Family DNA Polymerase in Action: A Mechanism for Error-Prone and Lesion-Bypass Replication. *Cell* **2001,** *107*, 91-102.
(85) Trincao, J.; Johnson, R. E.; Escalante, C. R.; Prakash, S.; Prakash, L.; Aggarwal, A. K. Structure of the Catalytic Core of *S. cerevisiae* DNA Polymerase Eta: Implications for Translesion DNA Synthesis. *Mol. Cell* **2001,** *8*, 417-426.
(86) Ummat, A.; Silverstein, T. D.; Jain, R.; Buku, A.; Johnson, R. E.; Prakash, L.; Prakash, S.; Aggarwal, A. K. Human DNA Polymerase Eta Is Pre-Aligned for dNTP Binding and Catalysis. *J. Mol. Biol.* **2012,** *415*, 627-634.
(87) Gaur, V.; Vyas, R.; Fowler, J. D.; Efthimiopoulos, G.; Feng, J. Y.; Suo, Z. Structural and Kinetic Insights into Binding and Incorporation of L-Nucleotide Analogs by a Y-Family DNA Polymerase. *Nucleic Acids Res.* **2014,** *42*, 9984-9995.
(88) Huang, H.; Chopra, R.; Verdine, G. L.; Harrison, S. C. Structure of a Covalently Trapped Catalytic Complex of HIV-1 Reverse Transcriptase: Implications for Drug Resistance. *Science* **1998,** *282*, 1669-1675.
(89) Kuchta, R. D.; Mizrahi, V.; Benkovic, P. A.; Johnson, K. A.; Benkovic, S. J. Kinetic Mechanism of DNA Polymerase I (Klenow). *Biochemistry* **1987,** *26*, 8410-8417.
(90) Patel, S. S.; Wong, I.; Johnson, K. A. Pre-Steady-State Kinetic Analysis of Processive DNA Replication Including Complete Characterization of an Exonuclease-Deficient Mutant. *Biochemistry* **1991,** *30*, 511-525.
(91) Zahurancik, W. J.; Klein, S. J.; Suo, Z. Kinetic Mechanism of DNA Polymerization Catalyzed by Human DNA Polymerase Epsilon. *Biochemistry* **2013,** *52*, 7041-7049.
(92) Brown, J. A.; Suo, Z. Elucidating the Kinetic Mechanism of DNA Polymerization Catalyzed by *Sulfolobus solfataricus* P2 DNA Polymerase B1. *Biochemistry* **2009,** *48*, 7502-7511.

(93) Fiala, K. A.; Suo, Z. Pre-Steady-State Kinetic Studies of the Fidelity of *Sulfolobus solfataricus* P2 DNA Polymerase IV. *Biochemistry* **2004,** *43*, 2106-2115.
(94) Fiala, K. A.; Suo, Z. Mechanism of DNA Polymerization Catalyzed by *Sulfolobus solfataricus* P2 DNA Polymerase IV. *Biochemistry* **2004,** *43*, 2116-2125.
(95) Donlin, M. J.; Patel, S. S.; Johnson, K. A. Kinetic Partitioning between the Exonuclease and Polymerase Sites in DNA Error Correction. *Biochemistry* **1991,** *30*, 538-546.
(96) Kati, W. M.; Johnson, K. A.; Jerva, L. F.; Anderson, K. S. Mechanism and Fidelity of HIV Reverse Transcriptase. *J. Biol. Chem.* **1992,** *267*, 25988-25997.
(97) Beard, W. A.; Wilson, S. H. Structure and Mechanism of DNA Polymerase Beta. *Chem. Rev.* **2006,** *106*, 361-382.
(98) Eger, B. T.; Benkovic, S. J. Minimal Kinetic Mechanism for Misincorporation by DNA Polymerase I (Klenow Fragment). *Biochemistry* **1992,** *31*, 9227-9236.
(99) Dahlberg, M. E.; Benkovic, S. J. Kinetic Mechanism of DNA Polymerase I (Klenow Fragment): Identification of a Second Conformational Change and Evaluation of the Internal Equilibrium Constant. *Biochemistry* **1991,** *30*, 4835-4843.
(100) Frey, M. W.; Sowers, L. C.; Millar, D. P.; Benkovic, S. J. The Nucleotide Analog 2-Aminopurine as a Spectroscopic Probe of Nucleotide Incorporation by the Klenow Fragment of *Escherichia coli* Polymerase I and Bacteriophage T4 DNA Polymerase. *Biochemistry* **1995,** *34*, 9185-9192.
(101) Hsieh, J. C.; Zinnen, S.; Modrich, P. Kinetic Mechanism of the DNA-Dependent DNA Polymerase Activity of Human Immunodeficiency Virus Reverse Transcriptase. *J. Biol. Chem.* **1993,** *268*, 24607-24613.
(102) Capson, T. L.; Peliska, J. A.; Kaboord, B. F.; Frey, M. W.; Lively, C.; Dahlberg, M.; Benkovic, S. J. Kinetic Characterization of the Polymerase and Exonuclease Activities of the Gene 43 Protein of Bacteriophage T4. *Biochemistry* **1992,** *31*, 10984-10994.
(103) Washington, M. T.; Prakash, L.; Prakash, S. Yeast DNA Polymerase Eta Utilizes an Induced-Fit Mechanism of Nucleotide Incorporation. *Cell* **2001,** *107*, 917-927.
(104) Washington, M. T.; Johnson, R. E.; Prakash, L.; Prakash, S. The Mechanism of Nucleotide Incorporation by Human DNA Polymerase Eta Differs from That of the Yeast Enzyme. *Mol. Cell. Biol.* **2003,** *23*, 8316-8322.
(105) Wohrl, B. M.; Krebs, R.; Goody, R. S.; Restle, T. Refined Model for Primer/Template Binding by HIV-1 Reverse Transcriptase: Pre-Steady-State Kinetic Analyses of Primer/Template Binding and Nucleotide Incorporation Events Distinguish between Different Binding Modes Depending on the Nature of the Nucleic Acid Substrate. *J. Mol. Biol.* **1999,** *292*, 333-344.
(106) Schermerhorn, K. M.; Gardner, A. F. Pre-Steady-State Kinetic Analysis of a Family D DNA Polymerase from *Thermococcus sp.* 9 Degrees N Reveals Mechanisms for Archaeal Genomic Replication and Maintenance. *J. Biol. Chem.* **2015,** *290*, 21800-21810.
(107) Lahiri, I.; Mukherjee, P.; Pata, J. D. Kinetic Characterization of Exonuclease-Deficient *Staphylococcus aureus* PolC, a C-Family Replicative DNA Polymerase. *PLoS One* **2013,** *8*, e63489.
(108) Einolf, H. J.; Guengerich, F. P. Kinetic Analysis of Nucleotide Incorporation by Mammalian DNA Polymerase Delta. *J. Biol. Chem.* **2000,** *275*, 16316-16322.
(109) Fiala, K. A.; Abdel-Gawad, W.; Suo, Z. Pre-Steady-State Kinetic Studies of the Fidelity and Mechanism of Polymerization Catalyzed by Truncated Human DNA Polymerase Lambda. *Biochemistry* **2004,** *43*, 6751-6762.

(110) Werneburg, B. G.; Ahn, J.; Zhong, X.; Hondal, R. J.; Kraynov, V. S.; Tsai, M. D. DNA Polymerase Beta: Pre-Steady-State Kinetic Analysis and Roles of Arginine-283 in Catalysis and Fidelity. *Biochemistry* **1996,** *35*, 7041-7050.
(111) Maxwell, B. A.; Suo, Z. Single-Molecule Investigation of Substrate Binding Kinetics and Protein Conformational Dynamics of a B-Family Replicative DNA Polymerase. *J. Biol. Chem.* **2013,** *288*, 11590-11600.
(112) Johnson, K. A. The Kinetic and Chemical Mechanism of High-Fidelity DNA Polymerases. *Biochim. Biophys. Acta* **2010,** *1804*, 1041-1048.
(113) McClure, W. R.; Jovin, T. M. The Steady State Kinetic Parameters and Non-Processivity of *Escherichia coli* Deoxyribonucleic Acid Polymerase I. *J. Biol. Chem.* **1975,** *250*, 4073-4080.
(114) Bryant, F. R.; Johnson, K. A.; Benkovic, S. J. Elementary Steps in the DNA Polymerase I Reaction Pathway. *Biochemistry* **1983,** *22*, 3537-3546.
(115) Liu, M. S.; Tsai, H. Y.; Liu, X. X.; Ho, M. C.; Wu, W. J.; Tsai, M. D. Structural Mechanism for the Fidelity Modulation of DNA Polymerase Lambda. *J. Am. Chem. Soc.* **2016,** *138*, 2389-2398.
(116) Ahn, J.; Kraynov, V. S.; Zhong, X.; Werneburg, B. G.; Tsai, M. D. DNA Polymerase Beta: Effects of Gapped DNA Substrates on dNTP Specificity, Fidelity, Processivity and Conformational Changes. *Biochem. J.* **1998,** *331 (Pt 1)*, 79-87.
(117) Brown, J. A.; Pack, L. R.; Sanman, L. E.; Suo, Z. Efficiency and Fidelity of Human DNA Polymerases Lambda and Beta During Gap-Filling DNA Synthesis. *DNA Repair (Amst)* **2011,** *10*, 24-33.
(118) Wu, W. J.; Su, M. I.; Wu, J. L.; Kumar, S.; Lim, L. H.; Wang, C. W.; Nelissen, F. H.; Chen, M. C.; Doreleijers, J. F.; Wijmenga, S. S.et al. How a Low-Fidelity DNA Polymerase Chooses Non-Watson-Crick from Watson-Crick Incorporation. *J. Am. Chem. Soc.* **2014,** *136*, 4927-4937.
(119) Ollis, D. L.; Brick, P.; Hamlin, R.; Xuong, N. G.; Steitz, T. A. Structure of Large Fragment of *Escherichia coli* DNA Polymerase I Complexed with dTMP. *Nature* **1985,** *313*, 762-766.
(120) Beese, L. S.; Friedman, J. M.; Steitz, T. A. Crystal Structures of the Klenow Fragment of DNA Polymerase I Complexed with Deoxynucleoside Triphosphate and Pyrophosphate. *Biochemistry* **1993,** *32*, 14095-14101.
(121) Chen, Y.; Zhang, J.; Liu, H.; Gao, Y.; Li, X.; Zheng, L.; Cui, R.; Yao, Q.; Rong, L.; Li, J.et al. Unique 5'-P Recognition and Basis for dG:dGTP Misincorporation of Asfv DNA Polymerase X. *PLoS Biol.* **2017,** *15*, e1002599.
(122) Nakane, S.; Ishikawa, H.; Nakagawa, N.; Kuramitsu, S.; Masui, R. The Structural Basis of the Kinetic Mechanism of a Gap-Filling X-Family DNA Polymerase That Binds Mg(2+)-dNTP before Binding to DNA. *J. Mol. Biol.* **2012,** *417*, 179-196.
(123) Kumar, S.; Bakhtina, M.; Tsai, M. D. Altered Order of Substrate Binding by DNA Polymerase X from African Swine Fever Virus. *Biochemistry* **2008,** *47*, 7875-7887.
(124) Maciejewski, M. W.; Shin, R.; Pan, B.; Marintchev, A.; Denninger, A.; Mullen, M. A.; Chen, K.; Gryk, M. R.; Mullen, G. P. Solution Structure of a Viral DNA Repair Polymerase. *Nat. Struct. Biol.* **2001,** *8*, 936-941.
(125) Showalter, A. K.; Tsai, M. D. A DNA Polymerase with Specificity for Five Base Pairs. *J. Am. Chem. Soc.* **2001,** *123*, 1776-1777.
(126) Brown, J. A.; Fowler, J. D.; Suo, Z. Kinetic Basis of Nucleotide Selection Employed by a Protein Template-Dependent DNA Polymerase. *Biochemistry* **2010,** *49*, 5504-5510.
(127) Nair, D. T.; Johnson, R. E.; Prakash, L.; Prakash, S.; Aggarwal, A. K. Rev1 Employs a Novel Mechanism of DNA Synthesis Using a Protein Template. *Science* **2005,** *309*, 2219-2222.

(128) Nelson, J. R.; Lawrence, C. W.; Hinkle, D. C. Deoxycytidyl Transferase Activity of Yeast Rev1 Protein. *Nature* **1996,** *382*, 729-731.
(129) Howell, C. A.; Prakash, S.; Washington, M. T. Pre-Steady-State Kinetic Studies of Protein-Template-Directed Nucleotide Incorporation by the Yeast Rev1 Protein. *Biochemistry* **2007,** *46*, 13451-13459.
(130) Chagovetz, A. M.; Sweasy, J. B.; Preston, B. D. Increased Activity and Fidelity of DNA Polymerase Beta on Single-Nucleotide Gapped DNA. *J. Biol. Chem.* **1997,** *272*, 27501-27504.
(131) Garcia-Diaz, M.; Bebenek, K.; Sabariegos, R.; Dominguez, O.; Rodriguez, J.; Kirchhoff, T.; Garcia-Palomero, E.; Picher, A. J.; Juarez, R.; Ruiz, J. F.et al. DNA Polymerase Lambda, a Novel DNA Repair Enzyme in Human Cells. *J. Biol. Chem.* **2002,** *277*, 13184-13191.
(132) Fiala, K. A.; Hypes, C. D.; Suo, Z. Mechanism of Abasic Lesion Bypass Catalyzed by a Y-Family DNA Polymerase. *J. Biol. Chem.* **2007,** *282*, 8188-8198.
(133) Brown, J. A.; Newmister, S. A.; Fiala, K. A.; Suo, Z. Mechanism of Double-Base Lesion Bypass Catalyzed by a Y-Family DNA Polymerase. *Nucleic Acids Res.* **2008,** *36*, 3867-3878.
(134) Maxwell, B. A.; Suo, Z. Kinetic Basis for the Differing Response to an Oxidative Lesion by a Replicative and a Lesion Bypass DNA Polymerase from *Sulfolobus solfataricus*. *Biochemistry* **2012,** *51*, 3485-3496.
(135) Kusumoto, R.; Masutani, C.; Shimmyo, S.; Iwai, S.; Hanaoka, F. DNA Binding Properties of Human DNA Polymerase Eta: Implications for Fidelity and Polymerase Switching of Translesion Synthesis. *Genes Cells* **2004,** *9*, 1139-1150.
(136) Ohashi, E.; Ogi, T.; Kusumoto, R.; Iwai, S.; Masutani, C.; Hanaoka, F.; Ohmori, H. Error-Prone Bypass of Certain DNA Lesions by the Human DNA Polymerase Kappa. *Genes Dev.* **2000,** *14*, 1589-1594.
(137) Woodgate, R. A Plethora of Lesion-Replicating DNA Polymerases. *Genes Dev.* **1999,** *13*, 2191-2195.
(138) Sherrer, S. M.; Brown, J. A.; Pack, L. R.; Jasti, V. P.; Fowler, J. D.; Basu, A. K.; Suo, Z. Mechanistic Studies of the Bypass of a Bulky Single-Base Lesion Catalyzed by a Y-Family DNA Polymerase. *J. Biol. Chem.* **2009,** *284*, 6379-6388.
(139) Gadkari, V. V.; Tokarsky, E. J.; Malik, C. K.; Basu, A. K.; Suo, Z. Mechanistic Investigation of the Bypass of a Bulky Aromatic DNA Adduct Catalyzed by a Y-Family DNA Polymerase. *DNA Repair (Amst)* **2014,** *21*, 65-77.
(140) Garcia-Gomez, S.; Reyes, A.; Martinez-Jimenez, M. I.; Chocron, E. S.; Mouron, S.; Terrados, G.; Powell, C.; Salido, E.; Mendez, J.; Holt, I. J.et al. Primpol, an Archaic Primase/Polymerase Operating in Human Cells. *Mol. Cell* **2013,** *52*, 541-553.
(141) Meng, X.; Zhou, Y.; Zhang, S.; Lee, E. Y.; Frick, D. N.; Lee, M. Y. DNA Damage Alters DNA Polymerase Delta to a Form That Exhibits Increased Discrimination against Modified Template Bases and Mismatched Primers. *Nucleic Acids Res.* **2009,** *37*, 647-657.
(142) Schmitt, M. W.; Matsumoto, Y.; Loeb, L. A. High Fidelity and Lesion Bypass Capability of Human DNA Polymerase Delta. *Biochimie* **2009,** *91*, 1163-1172.
(143) Higuchi, K.; Katayama, T.; Iwai, S.; Hidaka, M.; Horiuchi, T.; Maki, H. Fate of DNA Replication Fork Encountering a Single DNA Lesion During OriC Plasmid DNA Replication in Vitro. *Genes Cells* **2003,** *8*, 437-449.
(144) Johnson, K. A. *In 1 Transient-State Kinetic Analysis of Enzyme Reaction Pathways*; Academic Press, Inc.: San Diego, CA, 1992.

(145) Zahurancik, W. J.; Baranovskiy, A. G.; Tahirov, T. H.; Suo, Z. Comparison of the Kinetic Parameters of the Truncated Catalytic Subunit and Holoenzyme of Human DNA Polymerase Varepsilon. *DNA Repair (Amst)* **2015,** *29*, 16-22.
(146) Vande Berg, B. J.; Beard, W. A.; Wilson, S. H. DNA Structure and Aspartate 276 Influence Nucleotide Binding to Human DNA Polymerase Beta. Implication for the Identity of the Rate-Limiting Conformational Change. *J. Biol. Chem.* **2001,** *276*, 3408-3416.
(147) Brown, J. A.; Zhang, L.; Sherrer, S. M.; Taylor, J. S.; Burgers, P. M.; Suo, Z. Pre-Steady-State Kinetic Analysis of Truncated and Full-Length *Saccharomyces cerevisiae* DNA Polymerase Eta. *J. Nucleic Acids* **2010,** *2010*.
(148) Zhao, L.; Pence, M. G.; Eoff, R. L.; Yuan, S.; Fercu, C. A.; Guengerich, F. P. Elucidation of Kinetic Mechanisms of Human Translesion DNA Polymerase Kappa Using Tryptophan Mutants. *FEBS J.* **2014,** *281*, 4394-4410.
(149) Wong, J. H.; Fiala, K. A.; Suo, Z.; Ling, H. Snapshots of a Y-Family DNA Polymerase in Replication: Substrate-Induced Conformational Transitions and Implications for Fidelity of Dpo4. *J. Mol. Biol.* **2008,** *379*, 317-330.
(150) Lee, E.; Fowler, J. D.; Suo, Z.; Wu, Z. Backbone Assignment of the Binary Complex of the Full Length *Sulfolobus solfataricus* DNA Polymerase IV and DNA. *Biomol. NMR Assign.* **2017,** *11*, 39-43.
(151) Chu, X.; Liu, F.; Maxwell, B. A.; Wang, Y.; Suo, Z.; Wang, H.; Han, W.; Wang, J. Dynamic Conformational Change Regulates the Protein-DNA Recognition: An Investigation on Binding of a Y-Family Polymerase to Its Target DNA. *PLoS Comput. Biol.* **2014,** *10*, e1003804.
(152) Lone, S.; Townson, S. A.; Uljon, S. N.; Johnson, R. E.; Brahma, A.; Nair, D. T.; Prakash, S.; Prakash, L.; Aggarwal, A. K. Human DNA Polymerase Kappa Encircles DNA: Implications for Mismatch Extension and Lesion Bypass. *Mol. Cell* **2007,** *25*, 601-614.
(153) Moon, A. F.; Pryor, J. M.; Ramsden, D. A.; Kunkel, T. A.; Bebenek, K.; Pedersen, L. C. Sustained Active Site Rigidity During Synthesis by Human DNA Polymerase Mu. *Nat. Struct. Mol. Biol.* **2014,** *21*, 253-260.
(154) Lang, T.; Maitra, M.; Starcevic, D.; Li, S. X.; Sweasy, J. B. A DNA Polymerase Beta Mutant from Colon Cancer Cells Induces Mutations. *Proc. Natl. Acad. Sci. U. S. A.* **2004,** *101*, 6074-6079.
(155) Brown, J. A.; Pack, L. R.; Sherrer, S. M.; Kshetry, A. K.; Newmister, S. A.; Fowler, J. D.; Taylor, J. S.; Suo, Z. Identification of Critical Residues for the Tight Binding of Both Correct and Incorrect Nucleotides to Human DNA Polymerase Lambda. *J. Mol. Biol.* **2010,** *403*, 505-515.
(156) Garcia-Diaz, M.; Bebenek, K.; Krahn, J. M.; Blanco, L.; Kunkel, T. A.; Pedersen, L. C. A Structural Solution for the DNA Polymerase Lambda-Dependent Repair of DNA Gaps with Minimal Homology. *Mol. Cell* **2004,** *13*, 561-572.
(157) Wilson, S. H.; Kunkel, T. A. Passing the Baton in Base Excision Repair. *Nat. Struct. Biol.* **2000,** *7*, 176-178.
(158) Wang, J.; Sattar, A. K.; Wang, C. C.; Karam, J. D.; Konigsberg, W. H.; Steitz, T. A. Crystal Structure of a Pol Alpha Family Replication DNA Polymerase from Bacteriophage Rb69. *Cell* **1997,** *89*, 1087-1099.
(159) Kim, Y.; Eom, S. H.; Wang, J.; Lee, D. S.; Suh, S. W.; Steitz, T. A. Crystal Structure of *Thermus aquaticus* DNA Polymerase. *Nature* **1995,** *376*, 612-616.
(160) Kim, S. W.; Kim, D. U.; Kim, J. K.; Kang, L. W.; Cho, H. S. Crystal Structure of Pfu, the High Fidelity DNA Polymerase from *Pyrococcus furiosus. Int. J. Biol. Macromol.* **2008,** *42*, 356-361.

(161) Wynne, S. A.; Pinheiro, V. B.; Holliger, P.; Leslie, A. G. Structures of an Apo and a Binary Complex of an Evolved Archeal B Family DNA Polymerase Capable of Synthesising Highly Cy-Dye Labelled DNA. *PLoS One* **2013,** *8*, e70892.
(162) Rechkoblit, O.; Malinina, L.; Cheng, Y.; Kuryavyi, V.; Broyde, S.; Geacintov, N. E.; Patel, D. J. Stepwise Translocation of Dpo4 Polymerase During Error-Free Bypass of an OxoG Lesion. *PLoS Biol.* **2006,** *4*, e11.
(163) Brenlla, A.; Markiewicz, R. P.; Rueda, D.; Romano, L. J. Nucleotide Selection by the Y-Family DNA Polymerase Dpo4 Involves Template Translocation and Misalignment. *Nucleic Acids Res.* **2014,** *42*, 2555-2563.
(164) Johnson, S. J.; Taylor, J. S.; Beese, L. S. Processive DNA Synthesis Observed in a Polymerase Crystal Suggests a Mechanism for the Prevention of Frameshift Mutations. *Proc. Natl. Acad. Sci. U. S. A.* **2003,** *100*, 3895-3900.
(165) Basu, R. S.; Murakami, K. S. Watching the Bacteriophage N4 RNA Polymerase Transcription by Time-Dependent Soak-Trigger-Freeze X-Ray Crystallography. *J. Biol. Chem.* **2013,** *288*, 3305-3311.
(166) Bakhtina, M.; Roettger, M. P.; Kumar, S.; Tsai, M. D. A Unified Kinetic Mechanism Applicable to Multiple DNA Polymerases. *Biochemistry* **2007,** *46*, 5463-5472.
(167) Wang, M.; Lee, H. R.; Konigsberg, W. Effect of a and B Metal Ion Site Occupancy on Conformational Changes in an Rb69 DNA Polymerase Ternary Complex. *Biochemistry* **2009,** *48*, 2075-2086.
(168) Bakhtina, M.; Lee, S.; Wang, Y.; Dunlap, C.; Lamarche, B.; Tsai, M. D. Use of Viscogens, dNTPalphaS, and Rhodium(III) as Probes in Stopped-Flow Experiments to Obtain New Evidence for the Mechanism of Catalysis by DNA Polymerase Beta. *Biochemistry* **2005,** *44*, 5177-5187.
(169) Johnson, A. A.; Tsai, Y.; Graves, S. W.; Johnson, K. A. Human Mitochondrial DNA Polymerase Holoenzyme: Reconstitution and Characterization. *Biochemistry* **2000,** *39*, 1702-1708.
(170) Graves, S. W.; Johnson, A. A.; Johnson, K. A. Expression, Purification, and Initial Kinetic Characterization of the Large Subunit of the Human Mitochondrial DNA Polymerase. *Biochemistry* **1998,** *37*, 6050-6058.
(171) O'Donnell, M. E.; Kornberg, A. Complete Replication of Templates by *Escherichia coli* DNA Polymerase III Holoenzyme. *J. Biol. Chem.* **1985,** *260*, 12884-12889.
(172) Zahurancik, W. J.; Klein, S. J.; Suo, Z. Significant Contribution of the 3'-->5' Exonuclease Activity to the High Fidelity of Nucleotide Incorporation Catalyzed by Human DNA Polymerase. *Nucleic Acids Res.* **2014,** *42*, 13853-13860.
(173) Zhang, L.; Brown, J. A.; Newmister, S. A.; Suo, Z. Polymerization Fidelity of a Replicative DNA Polymerase from the Hyperthermophilic Archaeon *Sulfolobus solfataricus* P2. *Biochemistry* **2009,** *48*, 7492-7501.
(174) Joyce, C. M. How DNA Travels between the Separate Polymerase and 3'-5'-Exonuclease Sites of DNA Polymerase I (Klenow Fragment). *J. Biol. Chem.* **1989,** *264*, 10858-10866.
(175) Reha-Krantz, L. J. DNA Polymerase Proofreading: Multiple Roles Maintain Genome Stability. *Biochim. Biophys. Acta* **2010,** *1804*, 1049-1063.
(176) Fernandez-Leiro, R.; Conrad, J.; Yang, J. C.; Freund, S. M.; Scheres, S. H.; Lamers, M. H. Self-Correcting Mismatches During High-Fidelity DNA Replication. *Nat. Struct. Mol. Biol.* **2017,** *24*, 140-143.
(177) Ganai, R. A.; Bylund, G. O.; Johansson, E. Switching between Polymerase and Exonuclease Sites in DNA Polymerase Epsilon. *Nucleic Acids Res.* **2015,** *43*, 932-942.

(178) Johnson, A. A.; Johnson, K. A. Exonuclease Proofreading by Human Mitochondrial DNA Polymerase. *J. Biol. Chem.* **2001,** *276*, 38097-38107.
(179) Johnson, A. A.; Johnson, K. A. Fidelity of Nucleotide Incorporation by Human Mitochondrial DNA Polymerase. *J. Biol. Chem.* **2001,** *276*, 38090-38096.
(180) Johnson, S. J.; Beese, L. S. Structures of Mismatch Replication Errors Observed in a DNA Polymerase. *Cell* **2004,** *116*, 803-816.
(181) Xia, S.; Konigsberg, W. H. Mispairs with Watson-Crick Base-Pair Geometry Observed in Ternary Complexes of an Rb69 DNA Polymerase Variant. *Protein Sci.* **2014,** *23*, 508-513.
(182) Trincao, J.; Johnson, R. E.; Wolfle, W. T.; Escalante, C. R.; Prakash, S.; Prakash, L.; Aggarwal, A. K. Dpo4 Is Hindered in Extending a G.T Mismatch by a Reverse Wobble. *Nat. Struct. Mol. Biol.* **2004,** *11*, 457-462.
(183) Picher, A. J.; Garcia-Diaz, M.; Bebenek, K.; Pedersen, L. C.; Kunkel, T. A.; Blanco, L. Promiscuous Mismatch Extension by Human DNA Polymerase Lambda. *Nucleic Acids Res.* **2006,** *34*, 3259-3266.
(184) Batra, V. K.; Beard, W. A.; Pedersen, L. C.; Wilson, S. H. Structures of DNA Polymerase Mispaired DNA Termini Transitioning to Pre-Catalytic Complexes Support an Induced-Fit Fidelity Mechanism. *Structure* **2016,** *24*, 1863-1875.
(185) McCulloch, S. D.; Kunkel, T. A. The Fidelity of DNA Synthesis by Eukaryotic Replicative and Translesion Synthesis Polymerases. *Cell Res.* **2008,** *18*, 148-161.
(186) Osheroff, W. P.; Jung, H. K.; Beard, W. A.; Wilson, S. H.; Kunkel, T. A. The Fidelity of DNA Polymerase Beta During Distributive and Processive DNA Synthesis. *J. Biol. Chem.* **1999,** *274*, 3642-3650.
(187) Bebenek, K.; Garcia-Diaz, M.; Blanco, L.; Kunkel, T. A. The Frameshift Infidelity of Human DNA Polymerase Lambda. Implications for Function. *J. Biol. Chem.* **2003,** *278*, 34685-34690.
(188) Johnson, R. E.; Washington, M. T.; Prakash, S.; Prakash, L. Fidelity of Human DNA Polymerase Eta. *J. Biol. Chem.* **2000,** *275*, 7447-7450.
(189) Watson, J. D.; Crick, F. H. Genetical Implications of the Structure of Deoxyribonucleic Acid. *Nature* **1953,** *171*, 964-967.
(190) Loeb, L. A.; Kunkel, T. A. Fidelity of DNA Synthesis. *Annu. Rev. Biochem.* **1982,** *51*, 429-457.
(191) Kool, E. T.; Sintim, H. O. The Difluorotoluene Debate--a Decade Later. *Chem. Commun. (Camb.)* **2006,** *0*, 3665-3675.
(192) Kool, E. T. Hydrogen Bonding, Base Stacking, and Steric Effects in Dna Replication. *Annu. Rev. Biophys. Biomol. Struct.* **2001,** *30*, 1-22.
(193) Dzantiev, L.; Alekseyev, Y. O.; Morales, J. C.; Kool, E. T.; Romano, L. J. Significance of Nucleobase Shape Complementarity and Hydrogen Bonding in the Formation and Stability of the Closed Polymerase-DNA Complex. *Biochemistry* **2001,** *40*, 3215-3221.
(194) Lee, H. R.; Helquist, S. A.; Kool, E. T.; Johnson, K. A. Importance of Hydrogen Bonding for Efficiency and Specificity of the Human Mitochondrial DNA Polymerase. *J. Biol. Chem.* **2008,** *283*, 14402-14410.
(195) Xia, S.; Eom, S. H.; Konigsberg, W. H.; Wang, J. Structural Basis for Differential Insertion Kinetics of dNMPs Opposite a Difluorotoluene Nucleotide Residue. *Biochemistry* **2012,** *51*, 1476-1485.
(196) Xia, S.; Konigsberg, W. H. Rb69 DNA Polymerase Structure, Kinetics, and Fidelity. *Biochemistry* **2014,** *53*, 2752-2767.
(197) Kunkel, T. A.; Bebenek, K. DNA Replication Fidelity. *Annu. Rev. Biochem.* **2000,** *69*, 497-529.

(198) Nat. Commun.CRC Critical Reviews in BiochemistryWu, W.-J.; Yang, W.; Tsai, M.-D. How DNA Polymerases Catalyse Replication and Repair with Contrasting Fidelity. *Nat. Rev. Chem.* **2017,** *1*, 0068.
(199) Fiala, K. A.; Duym, W. W.; Zhang, J.; Suo, Z. Up-Regulation of the Fidelity of Human DNA Polymerase Lambda by Its Non-Enzymatic Proline-Rich Domain. *J. Biol. Chem.* **2006,** *281*, 19038-19044.
(200) Qin, Y.; Yang, Y.; Zhang, L.; Fowler, J. D.; Qiu, W.; Wang, L.; Suo, Z.; Zhong, D. Direct Probing of Solvent Accessibility and Mobility at the Binding Interface of Polymerase (Dpo4)-DNA Complex. *J. Phys. Chem. A* **2013,** *117*, 13926-13934.
(201) Wang, W.; Hellinga, H. W.; Beese, L. S. Structural Evidence for the Rare Tautomer Hypothesis of Spontaneous Mutagenesis. *Proc. Natl. Acad. Sci. U. S. A.* **2011,** *108*, 17644-17648.
(202) Bebenek, K.; Pedersen, L. C.; Kunkel, T. A. Replication Infidelity Via a Mismatch with Watson-Crick Geometry. *Proc. Natl. Acad. Sci. U. S. A.* **2011,** *108*, 1862-1867.
(203) Szymanski, E. S.; Kimsey, I. J.; Al-Hashimi, H. M. Direct NMR Evidence That Transient Tautomeric and Anionic States in dG•dT Form Watson-Crick-Like Base Pairs. *J. Am. Chem. Soc.* **2017,** *139*, 4326-4329.
(204) Kimsey, I. J.; Szymanski, E. S.; Zahurancik, W. J.; Shakya, A.; Xue, Y.; Chu, C. C.; Sathyamoorthy, B.; Suo, Z.; Al-Hashimi, H. M. Dynamic Basis for dG•dT Misincorporation Via Tautomerization and Ionization. *Nature* **2018,** *554*, 195-201.
(205) Batra, V. K.; Beard, W. A.; Shock, D. D.; Pedersen, L. C.; Wilson, S. H. Structures of DNA Polymerase Beta with Active-Site Mismatches Suggest a Transient Abasic Site Intermediate During Misincorporation. *Mol. Cell* **2008,** *30*, 315-324.
(206) Minnick, D. T.; Astatke, M.; Joyce, C. M.; Kunkel, T. A. A Thumb Subdomain Mutant of the Large Fragment of *Escherichia coli* DNA Polymerase I with Reduced DNA Binding Affinity, Processivity, and Frameshift Fidelity. *J. Biol. Chem.* **1996,** *271*, 24954-24961.
(207) Kiefer, J. R.; Mao, C.; Braman, J. C.; Beese, L. S. Visualizing DNA Replication in a Catalytically Active Bacillus DNA Polymerase Crystal. *Nature* **1998,** *391*, 304-307.
(208) Freudenthal, B. D.; Beard, W. A.; Wilson, S. H. DNA Polymerase Minor Groove Interactions Modulate Mutagenic Bypass of a Templating 8-Oxoguanine Lesion. *Nucleic Acids Res.* **2013,** *41*, 1848-1858.
(209) Spence, R. A.; Kati, W. M.; Anderson, K. S.; Johnson, K. A. Mechanism of Inhibition of HIV-1 Reverse Transcriptase by Nonnucleoside Inhibitors. *Science* **1995,** *267*, 988-993.
(210) Doublie, S.; Sawaya, M. R.; Ellenberger, T. An Open and Closed Case for All Polymerases. *Structure* **1999,** *7*, R31-35.
(211) Herschlag, D.; Piccirilli, J. A.; Cech, T. R. Ribozyme-Catalyzed and Nonenzymatic Reactions of Phosphate Diesters: Rate Effects Upon Substitution of Sulfur for a Nonbridging Phosphoryl Oxygen Atom. *Biochemistry* **1991,** *30*, 4844-4854.
(212) Arndt, J. W.; Gong, W.; Zhong, X.; Showalter, A. K.; Liu, J.; Dunlap, C. A.; Lin, Z.; Paxson, C.; Tsai, M. D.; Chan, M. K. Insight into the Catalytic Mechanism of DNA Polymerase Beta: Structures of Intermediate Complexes. *Biochemistry* **2001,** *40*, 5368-5375.
(213) Luo, G.; Wang, M.; Konigsberg, W. H.; Xie, X. S. Single-Molecule and Ensemble Fluorescence Assays for a Functionally Important Conformational Change in T7 DNA Polymerase. *Proc. Natl. Acad. Sci. U. S. A.* **2007,** *104*, 12610-12615.
(214) Lee, H. R.; Wang, M.; Konigsberg, W. The Reopening Rate of the Fingers Domain Is a Determinant of Base Selectivity for Rb69 DNA Polymerase. *Biochemistry* **2009,** *48*, 2087-2098.

(215) Kirmizialtin, S.; Nguyen, V.; Johnson, K. A.; Elber, R. How Conformational Dynamics of DNA Polymerase Select Correct Substrates: Experiments and Simulations. *Structure* **2012,** *20*, 618-627.
(216) Kellinger, M. W.; Johnson, K. A. Nucleotide-Dependent Conformational Change Governs Specificity and Analog Discrimination by HIV Reverse Transcriptase. *Proc. Natl. Acad. Sci. U. S. A.* **2010,** *107*, 7734-7739.
(217) Kellinger, M. W.; Johnson, K. A. Role of Induced Fit in Limiting Discrimination against AZT by HIV Reverse Transcriptase. *Biochemistry* **2011,** *50*, 5008-5015.
(218) Yang, W. An Overview of Y-Family DNA Polymerases and a Case Study of Human DNA Polymerase Eta. *Biochemistry* **2014,** *53*, 2793-2803.
(219) Beckman, J. W.; Wang, Q.; Guengerich, F. P. Kinetic Analysis of Correct Nucleotide Insertion by a Y-Family DNA Polymerase Reveals Conformational Changes Both Prior to and Following Phosphodiester Bond Formation as Detected by Tryptophan Fluorescence. *J. Biol. Chem.* **2008,** *283*, 36711-36723.
(220) Fiala, K. A.; Sherrer, S. M.; Brown, J. A.; Suo, Z. Mechanistic Consequences of Temperature on DNA Polymerization Catalyzed by a Y-Family DNA Polymerase. *Nucleic Acids Res.* **2008,** *36*, 1990-2001.
(221) Eoff, R. L.; Sanchez-Ponce, R.; Guengerich, F. P. Conformational Changes During Nucleotide Selection by *Sulfolobus solfataricus* DNA Polymerase Dpo4. *J. Biol. Chem.* **2009,** *284*, 21090-21099.
(222) Vyas, R.; Reed, A. J.; Raper, A. T.; Zahurancik, W. J.; Wallenmeyer, P. C.; Suo, Z. Structural Basis for the D-Stereoselectivity of Human DNA Polymerase Beta. *Nucleic Acids Res.* **2017,** *45*, 6228-6237.
(223) Vyas, R.; Zahurancik, W. J.; Suo, Z. Structural Basis for the Binding and Incorporation of Nucleotide Analogs with L-Stereochemistry by Human DNA Polymerase Lambda. *Proc. Natl. Acad. Sci. U. S. A.* **2014,** *111*, E3033-3042.
(224) Shock, D. D.; Freudenthal, B. D.; Beard, W. A.; Wilson, S. H. Modulating the DNA Polymerase Beta Reaction Equilibrium to Dissect the Reverse Reaction. *Nat. Chem. Biol.* **2017,** *13*, 1074-1080.
(225) Raper, A. T.; Reed, A. J.; Gadkari, V. V.; Suo, Z. Advances in Structural and Single-Molecule Methods for Investigating DNA Lesion Bypass and Repair Polymerases. *Chem. Res. Toxicol.* **2017,** *30*, 260-269.
(226) Brown, J. A.; Duym, W. W.; Fowler, J. D.; Suo, Z. Single-Turnover Kinetic Analysis of the Mutagenic Potential of 8-Oxo-7,8-Dihydro-2'-Deoxyguanosine During Gap-Filling Synthesis Catalyzed by Human DNA Polymerases Lambda and Beta. *J. Mol. Biol.* **2007,** *367*, 1258-1269.
(227) Bedford, E.; Tabor, S.; Richardson, C. C. The Thioredoxin Binding Domain of Bacteriophage T7 DNA Polymerase Confers Processivity on *Escherichia coli* DNA Polymerase I. *Proc. Natl. Acad. Sci. U. S. A.* **1997,** *94*, 479-484.
(228) Beard, W. A.; Wilson, S. H. Structural Insights into the Origins of DNA Polymerase Fidelity. *Structure* **2003,** *11*, 489-496.
(229) Ohmori, H.; Friedberg, E. C.; Fuchs, R. P.; Goodman, M. F.; Hanaoka, F.; Hinkle, D.; Kunkel, T. A.; Lawrence, C. W.; Livneh, Z.; Nohmi, T.et al. The Y-Family of DNA Polymerases. *Mol. Cell* **2001,** *8*, 7-8.
(230) Lehmann, A. R.; Niimi, A.; Ogi, T.; Brown, S.; Sabbioneda, S.; Wing, J. F.; Kannouche, P. L.; Green, C. M. Translesion Synthesis: Y-Family Polymerases and the Polymerase Switch. *DNA Repair (Amst)* **2007,** *6*, 891-899.

(231) Matsuda, T.; Bebenek, K.; Masutani, C.; Hanaoka, F.; Kunkel, T. A. Low Fidelity DNA Synthesis by Human DNA Polymerase-Eta. *Nature* **2000,** *404*, 1011-1013.
(232) Pecoraro, V. L.; Hermes, J. D.; Cleland, W. W. Stability Constants of Mg^{2+} and Cd^{2+} Complexes of Adenine Nucleotides and Thionucleotides and Rate Constants for Formation and Dissociation of MgATP and MgADP. *Biochemistry* **1984,** *23*, 5262-5271.
(233) Roettger, M. P.; Fiala, K. A.; Sompalli, S.; Dong, Y.; Suo, Z. Pre-Steady-State Kinetic Studies of the Fidelity of Human DNA Polymerase Mu. *Biochemistry* **2004,** *43*, 13827-13838.
(234) Oertell, K.; Harcourt, E. M.; Mohsen, M. G.; Petruska, J.; Kool, E. T.; Goodman, M. F. Kinetic Selection Vs. Free Energy of DNA Base Pairing in Control of Polymerase Fidelity. *Proc. Natl. Acad. Sci. U. S. A.* **2016,** *113*, E2277-2285.
(235) Hanes, J. W.; Johnson, K. A. A Novel Mechanism of Selectivity against AZT by the Human Mitochondrial DNA Polymerase. *Nucleic Acids Res.* **2007,** *35*, 6973-6983.
(236) Nami, F.; Gast, P.; Groenen, E. J. Rapid Freeze-Quench EPR Spectroscopy: Improved Collection of Frozen Particles. *Appl. Magn. Reson.* **2016,** *47*, 643-653.